(12) 01

LEVEL II

(6) HOLOGRAPHIC LENS FOR PILOT'S HEAD UP DISPLAY PHASE IV.

(10) A./Au, A./Graube, L.G./Cook

Hughes Research Laboratories

3011 Malibu Canyon Road

Malibu, CA 90265

(11) Aug[illegible]978 (13) 67p.

(15) Contract N62269-76-C-0188

(9) Final Report,

For period 25 Mar[illegible]76 [illegible] 25 Mar[illegible]77,

Approved for public release. Distribution unlimited.

(18) NADC

Prepared for

NAVAL AIR DEVELOPMENT CENTER

Warminster, PA 18974

(19) 78-191-60

UNCLASSIFIED

SECURITY CLASSIFICATION OF THIS PAGE (When Data Entered)

REPORT DOCUMENTATION PAGE		READ INSTRUCTIONS BEFORE COMPLETING FORM
1. REPORT NUMBER NADC 78-191-60	2. GOVT ACCESSION NO.	3. RECIPIENT'S CATALOG NUMBER
4. TITLE (and Subtitle) Holographic Lens for Pilot's Head Up Display - Phase IV		5. TYPE OF REPORT & PERIOD COVERED Final Technical Report 25 March 1976 - 25 March 1977 6. PERFORMING ORG. REPORT NUMBER
7. AUTHOR(s) A. Au, A. Graube, L. G. Cook		8. CONTRACT OR GRANT NUMBER(s) N62269-76-C-0188
9. PERFORMING ORGANIZATION NAME AND ADDRESS Hughes Research Laboratories 3011 Malibu Canyon Road, Malibu, CA 90265		10. PROGRAM ELEMENT, PROJECT, TASK AREA & WORK UNIT NUMBERS
11. CONTROLLING OFFICE NAME AND ADDRESS Air Vehicle Technology Dept. (30421) Naval Air Development Center Warminster, PA 18974		12. REPORT DATE August 1978 13. NUMBER OF PAGES 71
14. MONITORING AGENCY NAME & ADDRESS(if different from Controlling Office)		15. SECURITY CLASS. (of this report) Unclassified 15a. DECLASSIFICATION DOWNGRADING SCHEDULE

16. DISTRIBUTION STATEMENT (of this Report)

Approved for public release. Distribution unlimited.

17. DISTRIBUTION STATEMENT (of the abstract entered in Block 20, if different from Report)

18. SUPPLEMENTARY NOTES

19. KEY WORDS (Continue on reverse side if necessary and identify by block number)

HEAD-UP DISPLAY, DICHROMATED GELATIN, REFLECTION HOLOGRAM, STABILITY CONTROL AND MONITOR SYSTEM, HOLOGRAM ENVIRONMENTAL TEST, REFLECTION HOLOGRAM OPTICAL DESIGN, HOLOGRAPHIC LENS

20. ABSTRACT (Continue on reverse side if necessary and identify by block number)

This report describes work done under Contract N62269-76-C-0188 to design and fabricate a holographic lens for pilot's head up display. A holographic head up display (HHUD) trade-off study was done to minimize weight and size of the HHUD. This led to a design for a 25° H x 18° V FOV system with a 3.5 in. (89 mm) circular exit pupil at an eye relief of 26 in. (660 mm). A new design concept was used to

(cont)

DD FORM 1 JAN 73 1473 EDITION OF 1 NOV 65 IS OBSOLETE

UNCLASSIFIED

SECURITY CLASSIFICATION OF THIS PAGE (When Data Entered)

20. ABSTRACT (Continued)

reduce the complexity of the relay lens system to a five element asymmetric design. Final system optimization reduced typical errors to 2-5 mrad. Relayless HHUD and holographic relay lens designs were investigated and found to provide moderate FOV and performance, limited by uncorrected hologram aberrations.

A relayless HHUD design was used as a basis for fabricating a 36° off axis, symmetric reflection hologram lens on an 8 in. x 10 in. (200 mm x 250 mm) substrate. The system was designed for a ∿14° circular FOV with a 3 in. (75 mm) circular exit pupil at an eye relief of 21.3 in. (540 mm). Residual aberrations of the system lead to ∿3 mrad maximum accuracy error and ∿1.5 mrad average binocular disparity error.

The construction beam optical systems for this relayless HHUD design were implemented with modifications of the existing NADC recording facility. Exposure wavelength was 5145 A from an argon ion laser. Stability control and monitoring systems maintained better than λ/20 stability for 30 minute exposure times. Hologram efficiency of 75% was measured at 5430 A, the dominant wavelength of the P-43 phosphor.

Tests confirmed the ability of holographic lenses to withstand cockpit environments. Holographic lenses protected by clear adhesive and cover glass were exposed to sunlight for 14 months, 100% relative humidity for 4 hours, and 80°C temperature for over 720 hours. No degradation of diffraction efficiency, peak reflective wavelength, light scattering, or absorption loss, was observed.

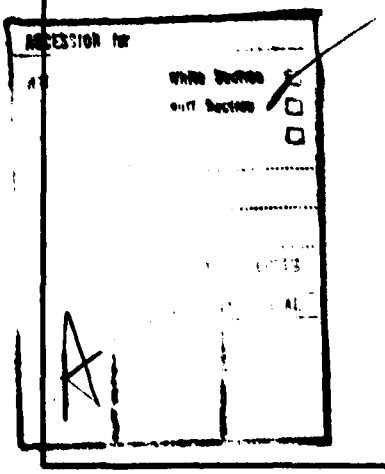

TABLE OF CONTENTS

LIST OF ILLUSTRATIONS

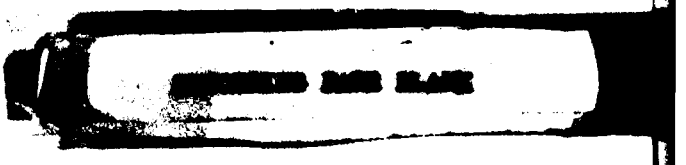

PREFACE

This final report covers the work accomplished during the period 25 March 1976 through 25 March 1977 under Contract N62269-76-C-0188, "Holographic Lens for Pilot's Head-Up Display (Phase 4)." This work was supported by the Naval Air Systems Command under the guidance of Mr. George Tsaparas and Mr. William B. King. This program is under the technical direction of Mr. Wally Freitag and Mr. Harold Green of the Naval Air Development Center, Warminster, Pennsylvania.

The work was accomplished by the Exploratory Studies Department of the Hughes Research Laboratories, a Division of the Hughes Aircraft Company, under the direction of Dr. Donald H. Close. The technical work was directed by Mr. Anson Au, the program manager. Mr. Andrejs Graube provided optimal processing techniques. Mr. Angel F. Baneulos assisted in material preparation. Mr. Cesar C. DeAnda performed many of the tasks in assembling the hologram recording apparatus and fabricating the holographic lens. Dr. Alexis C. Livanos provided valuable support in all technical areas. The design trade-off study and optical design of the reflection HHUD systems were performed by Mr. Lacy G. Cook and Dr. Roger J. Withrington of the Electro-Optics Department. Mr. Gaylord E. Moss acted as consultant to the program.

SECTION 1

INTRODUCTION AND PROGRAM SUMMARY

A. INTRODUCTION

This is the final technical report on Contract N62269-76-C-0188, Phase 4 of the Naval Air Development Center (NADC) program to develop a holographic lens for pilot's head-up display (HUD). The work covered by this report was performed at Hughes Research Laboratories (HRL), Malibu, California during the period 25 March 1976 to 25 March 1977.

The objective of the NADC program is to develop a HUD system meeting the optical system parameters and performance goals stated in the NADC "Specification for Hologram Lens System."[1] The basic system parameters are a 25° field of view (FOV), an exit pupil 3 in. high by 5 in. wide, and an eye relief of 25 in. In Phase 1, preliminary system design and recording material optimization led to a demonstration of high quality holographic HUD imagery with a half-size transmission hologram configuration having a 40° off-axis angle.[2] In Phase 2, we designed and fabricated a dynamically stabilized recording system with symmetric 50° off-axis construction beams for exposing the full-scale transmission hologram.[3] In Phase 3, a full-scale transmission holographic lens (16-in. diameter) was successfully recorded in dye-sensitized dichromated gelatin.[4]

In this Phase 4, the subject of this report, trade-off studies were performed to minimize weight and size of holographic HUD (HHUD) systems using flat, reflective hologram lenses. A relayless 36° off-axis, symmetric reflection HHUD was designed and fabricated for use at 5430 Å with a P43 phosphor cathode-ray tube (CRT) in the NADC advanced integrated display system (AIDS) demonstrator. The existing NADC hologram recording facility was modified to record the ∿8-in.-diameter holographic lens. Environmental tests consisting of long-duration exposure to sunlight, 100% relative humidity, and high temperature were conducted.

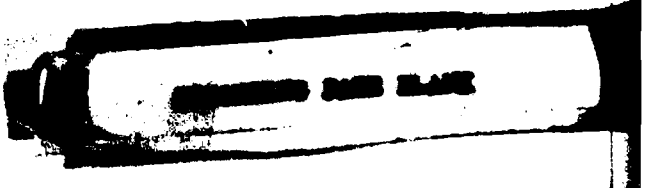

B. PROGRAM SUMMARY

1. HHUD Trade-Off Study

A HHUD was designed to fit within the limiting lines of the AIDS demonstrator cockpit. Characteristics of the HHUD system are 25° H x 18° V FOV with an exit pupil of 3.5 in. at an eye relief of 26 in. It was necessary to reduce the vertical FOV to fit the display into the cockpit. Reducing the exit pupil and vertical FOV resulted in smaller relay lens elements. The 45° off-axis holographic lens has a focal length of 10.5 in. The relay system has a five-element, asymmetric lens design optimized to cancel aberrations of the holographic lens. Final system optimization resulted in typical errors of 2 to 5 mrad.

Relayless HHUD geometries can provide moderate FOV and performance, limited by uncorrected hologram aberration. Short-focal-length lenses offer large FOV but suffer from large image errors. Long-focal-length lenses offer improved performance with reduced FOV. A 15-in. focal length, 50° off-axis relayless flat plate HHUD has ∿8 mrad of axial coma.

The prospect of using a holographic relay lens was investigated by developing a design using two flat plate reflective holograms of nearly equal power with a cylindrical field lens. The display has a 16° H x 12.8° V with a 3-in. exit pupil at a 29 in. eye relief. Moderate performance was achieved with axial accuracy error of 4 mrad.

2. HHUD (Demonstrator) Design and Specification

A relayless HUD system was designed for moderate FOV and performance without conforming to the rigid geometry requirements of a fighter cockpit. This design was used to fabricate a reflective holographic lens to illustrate its properties and operation. The relayless system was designed for 14° circular FOV with a 3 in. circular exit pupil at an eye relief of 21.3 in. The focal length of the 36° off-axis, symmetric reflection hologram lens is 20 in. Aberrations of the system are ∿3 mrad maximum accuracy error and ∿1.5 mrad average disparity error.

3. Fabrication and Testing of the Reflection Hologram

The 36° off-axis reflection holographic lens of the relayless HHUD design was recorded in dichromated gelatin on an 8 in. x 10 in. substrate. Modifications of the existing NADC hologram recording facility included construction hardware design and fabrication and conversion of the krypton ion laser source to argon to use the exposure wavelength of 5145 Å. Construction beam optical systems were assembled on the granite optical table within an acoustic enclosure. Stability control and monitoring systems were improved to maintain recording stability to better than $\lambda/20$ for 30-min. exposure time. Hologram efficiency of 75% was measured at 5430 Å, operating wavelength of the P43 phosphor CRT.

4. Reflection Hologram Environmental Test

Holographic lenses protected by clear adhesive and cover glass were tested by exposure to sunlight, 100% relative humidity, and high temperature. The performance parameters assessed were diffraction efficiency, peak reflective wavelength, and light scattering or absorption loss. Exposure to sunlight for 14 months and to 100% humidity for 4 hr did not degrade the hologram's optical properties. Hologram lens performance was not affected when exposed to 80°C for over 720 hr. Destructive testing showed that hologram lenses can withstand high temperatures (up to 100°C). These environmental tests confirm the ability of HHUD lenses to withstand cockpit environments.

SECTION 2

HHUD TRADE-OFF STUDIES

One result of Phase 3 was the design of a HHUD using a flat-plate reflective holographic lens. Although this design was not constrained to any aircraft cockpit geometry, it did serve as a reference point in establishing the useful range and probable performance of a display using such a holographic lens. Building on the knowledge and experience gained during Phase 3, the goals for Phase 4 included the design of another HHUD. In designing it, the following guidelines were followed:

- The display should have a flat plate reflection holographic lens.
- It should conform to the geometry of the AIDS demonstrator cockpit.
- The size and complexity of the relay lens should be reduced as much as possible.

This section documents the optical design work done in Phase 4. The current HHUD design is briefly summarized in this introduction, and the details are presented in Section 2.A. Section 2.B. reports the performance of this display. Where it is useful, comparisons are made with the Phase 3 design. Section 2.D. presents the design and performance of a relayless HHUD that uses two flat-plate reflective holographic lenses. This design gives considerable insight into the performance generally to be expected from a display that does not have a relay lens for aberration correction. Section 3 describes the optical design and performance of the reflective holographic lens that was fabricated as part of the Phase 4 program.

A. OPTICAL DESIGN

The Phase 4 HHUD is shown in Figures 1 and 2, along with the critical limiting lines of the AIDS demonstrator cockpit. The optical characteristics of the design are given in Table 1. There are many things about this design which differ from the Phase 3 design; indeed

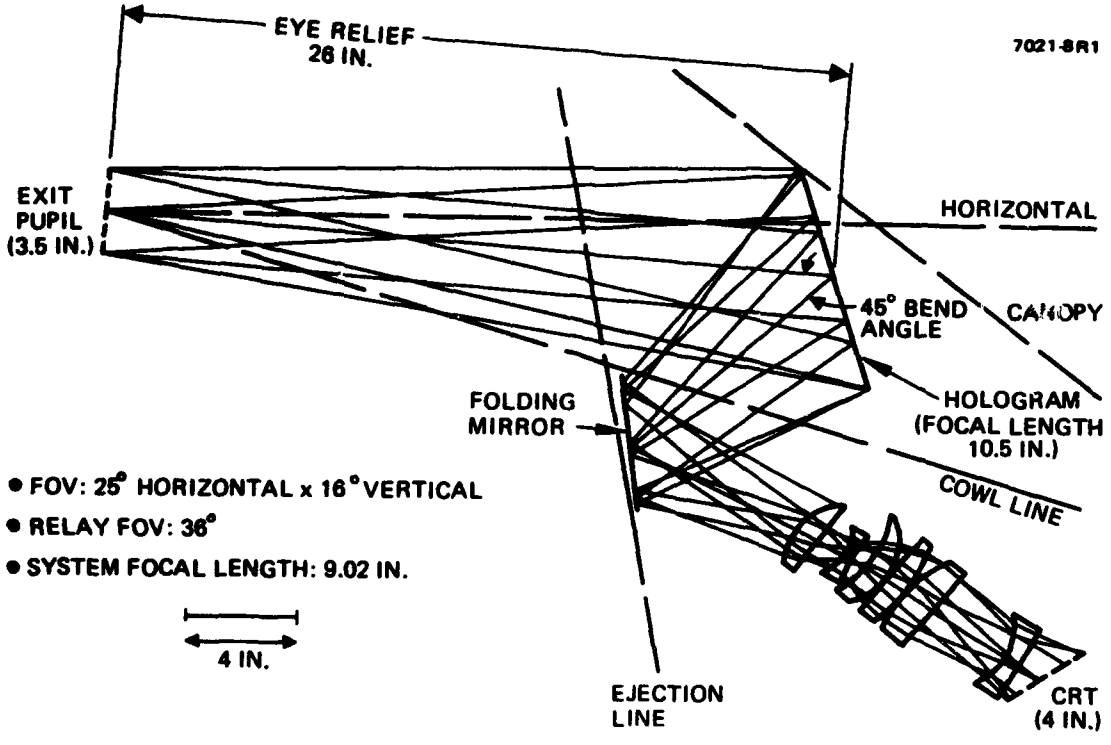

Figure 1. Vertical section of Phase 4 HHUD and critical boundaries of AIDS demonstrator cockpit.

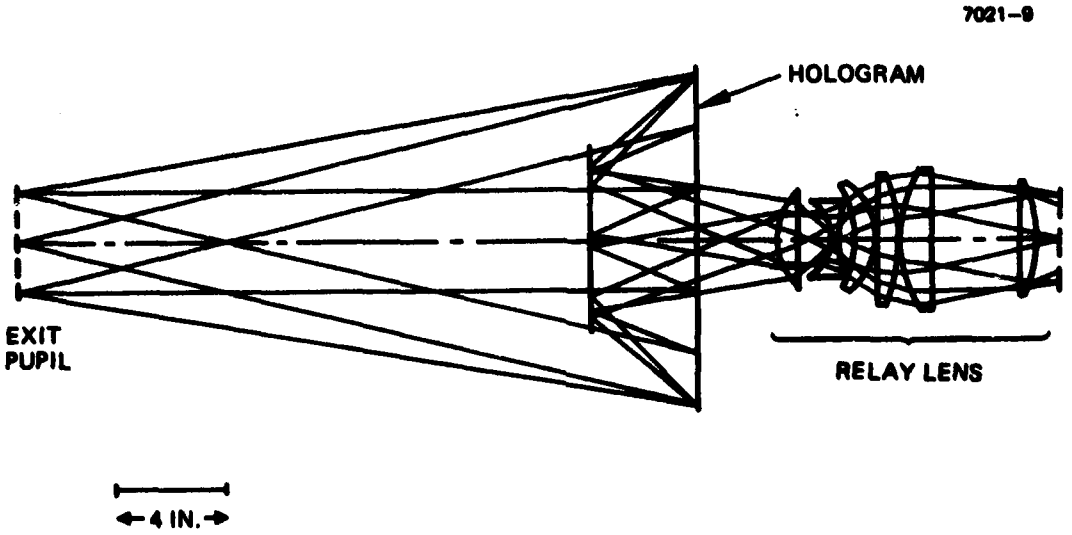

Figure 2. Horizontal section of Phase 4 HHUD.

even some aspects of the design approach have changed. These differences resulted from the three major guidelines listed above. The holographic lens has a shorter focal length and a smaller horizontal exit pupil diameter. The vertical FOV was to allow the combiner to fit the cockpit, and the relay lens was completely redesigned to meet the new requirements. Table 2 summarizes the performance of the design (in terms of binocular disparity and accuracy errors) for various parts of the FOV. This design performs comparably to the Phase 3 design. (See Section 2.B.)

Table 1. Comparison of the Optical Characteristics of the Phase 3 and Phase 4 Designs.

Characteristic	Phase 4	Phase 3
CRT size, in.	4	4
Total FOV, deg.	25 H x 18 V	25 H x 25 V
Maximum monocular FOV, deg.	25 H x 16 V	25 H x 25 V
System focal length, in.	9.02[a]	9.02[a]
System f/no.	2.58	1.80
Maximum pupil diameter, in.	3.5	5.0
Hologram, focal length, in.	10.5	14.9
Bend angle, deg.	45	43
Hologram f/no.	3.0	3.0
Eye relief, in.	26	25
Relay magnification	1.16 X	1.66 X
Relay f/no.	1.39	1.13
Relay FOV, deg.	36	17

[a]Average.

6029

Table 2. Performance Summary for Phase 4 HHUD (Errors Quoted Are Maxima).

Field Angle[a]	Pupil Position (Y), in.	Accuracy Error, mrad	Binocular Disparity, mrad	
			Horizontal	Vertical
$\alpha = 0°$	Y = 1	3	4	0
	Y = 0[b]	1.5	5	0
	Y = -1	3	8	0
$\alpha = 5.5°$	Y = 1	5	8	0
	Y = 0	3.5	7	0
	Y = -1	1	1	0
$\alpha = 5.5°$	Y = 1	7	10	0
	Y = 0	2.5	3.5	0
	Y = -1	2	4	0
$\beta = 5.5°$	Y = 1	5	11	13
	Y = 0	0.5	4	6
	Y = -1	3	7	7
$\alpha = 8°$	Y = 1	-	-	-
	Y = 0	0.5	6	0
	Y = -1	8	19	0
$\alpha = 8°$	Y = 1	4	10	0
	Y = 0	0.5	4	0
	Y = -1	-	-	-
$\beta = 8°$	Y = 1	10	15	19
	Y = 0	2.5	4	4
	Y = -1	1.5	5	3
$\beta = 12.5°$	Y = 1	9[c]	-	-
	Y = 0	13[c]	-	-
	Y = -1	7[c]	-	-

[a] α = vertical field angle
β = horizontal field angle
Y = vertical pupil dimension

[b] Center

[c] Monocular

6029

Figure 3 illustrates the problems associated with fitting the display to the AIDS demonstration cockpit by showing the Phase 3 design laid over the pertinent lines of the cockpit. This section is broken into three subsections: system considerations, the holographic lens, and the relay lens.

1. System Considerations

The CRT size (4 in.) and the horizontal FOV (25°) are unchanged from their Phase 3 values and therefore the system focal length is unchanged at 9.02 in. The horizontal diameter of the exit pupil has been reduced from 5 in. to 3.5 in., giving a system speed of 2.58. This change was necessary to maintain reasonable hologram and relay lens speeds, as will be discussed later. The effect of the reduction on system performance can accurately be gauged by referring to JANAIR report 680712 on visual requirements for HUDs, in which it is shown that pilot reaction time (the time necessary to locate and react to the displayed information) is not significantly increased when the display exit pupil is reduced from a 3-in. by 5-in. rectangle to a 3-in.-diameter circle.

To fit the cockpit, the vertical FOV was reduced to an instantaneous value of 16°. The total vertical FOV is ~18°, depending on the relay lens and folding mirror sizes and on distortion. Limitations on the size of the hologram cause some vignetting of the pupil at the extremes of the FOV. At +8° vertical, the top half of the exit pupil is not used; at -8° vertical, the bottom half is not used. At +12.5° horizontal, the left half of the pupil is vignetted, and the right half is vignetted at -12.5° horizontal.

2. Hologram Design

To fit the system into the allowed cockpit area, the hologram focal length was chosen to be 10.5 in. The 3.5 in. exit pupil gives a hologram speed of 3.00. The cut in focal length makes the current focal length shorter than that of the Phase 3 hologram by 4.40 in. and shortens the hologram-to-entrance pupil distance by approximately 19 in.

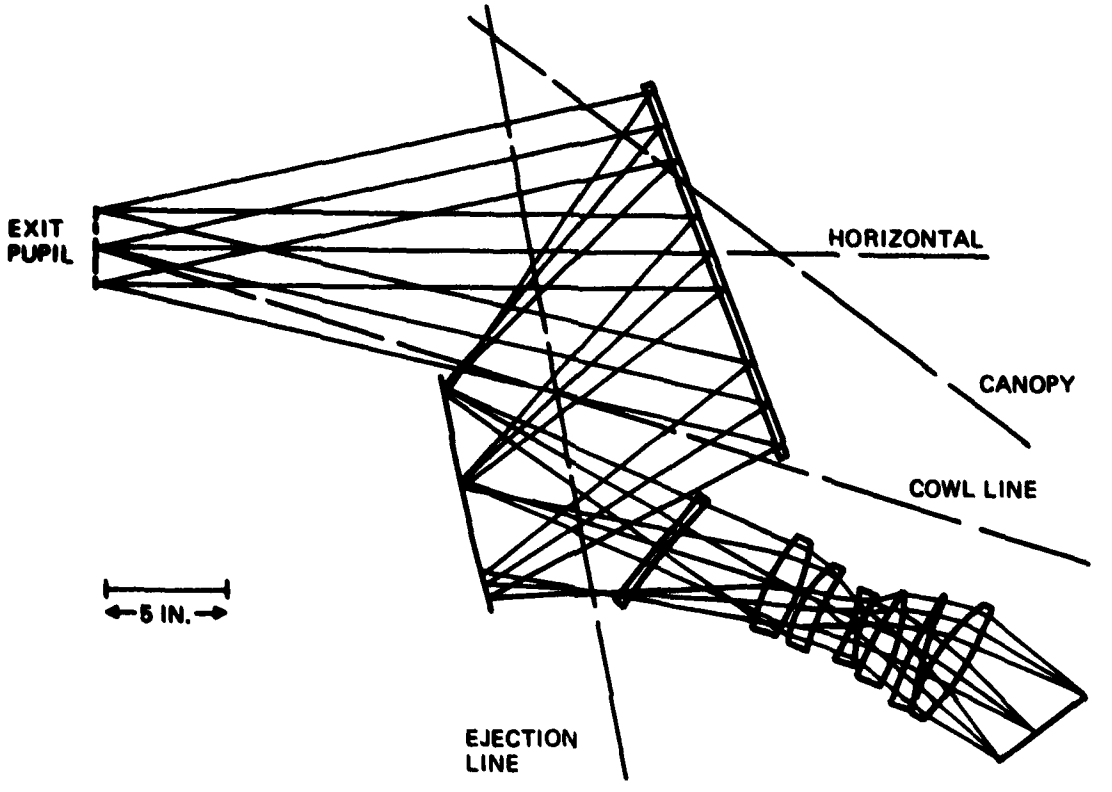

Figure 3. Phase 3 design viewed against the lines of the AIDS demonstrator cockpit. To fit within the canopy, the vertical FOV and extent of the hologram must be reduced. To fit within the ejection line, the hologram focal length must be reduced and bend angle increased so that the fold mirror can be moved forward.

Shortening the distance to the entrance pupil decreases its size relative to the exit pupil. This, the reduction in exit pupil size, and the decrease in vertical FOV result in smaller-sized relay lens elements.

From the Phase 3 trade-off information for a flat-plate hologram of 10.5 in. focal length and 45° bend angle, one would expect such a hologram to have these properties:[4]

- Image tilt disparity of ∿20°.
- Axial coma of ∿25 mrads and variation of coma across the FOV.
- Variation in field curvatures.

The Phase 3 trade-off study and design were done for holograms constructed using spherical wavefronts originating from point sources located at the hologram entrance and exit pupils. This construction geometry produces the widest FOV because the chief rays are reconstructed with maximum efficiency. The aberrations inherent in this design approach were studied fully during Phase 3. For the present design, we utilized aberrated construction wavefronts to simplify the design of the relay lens. These aberrated wavefronts were produced by introducing a single cylindrical lens into each construction beam. The optimization capability of the raytrace design program was used to minimize the image tilt disparity.[4]

The Phase 4 hologram is described in Table 1. Its geometrical aberrations are plotted in Figure 4, and its diffraction efficiency across the pupil and FOV are shown in Figure 5. The construction geometry for this hologram is shown in Figure 6. In contrast to the properties predicted in the Phase 3 trade-off curves, this hologram has

- No image tilt disparity
- Axial coma of ∿13 mrad.

Field curvature problems eventually required that a cylindrical field lens be added to the relay during the system optimization.

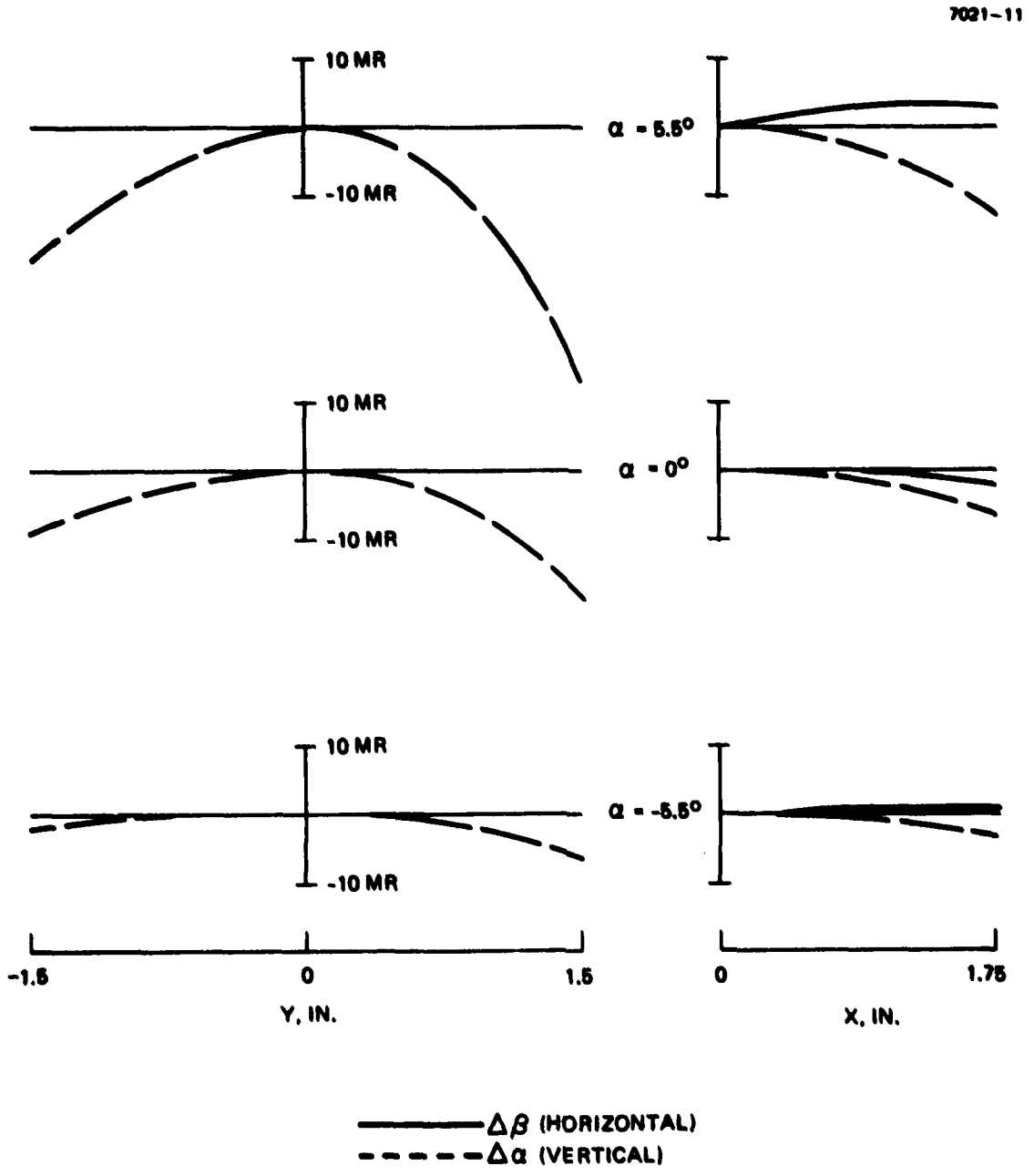

Figure 4. Geometrical aberrations of the Phase 4 hologram.

7021-12

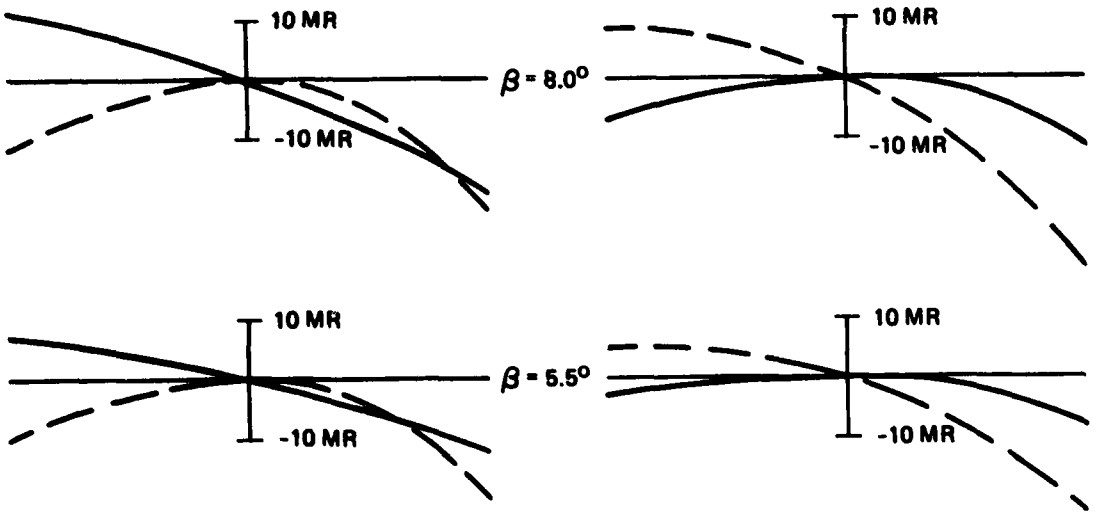

Figure 4. Continued.

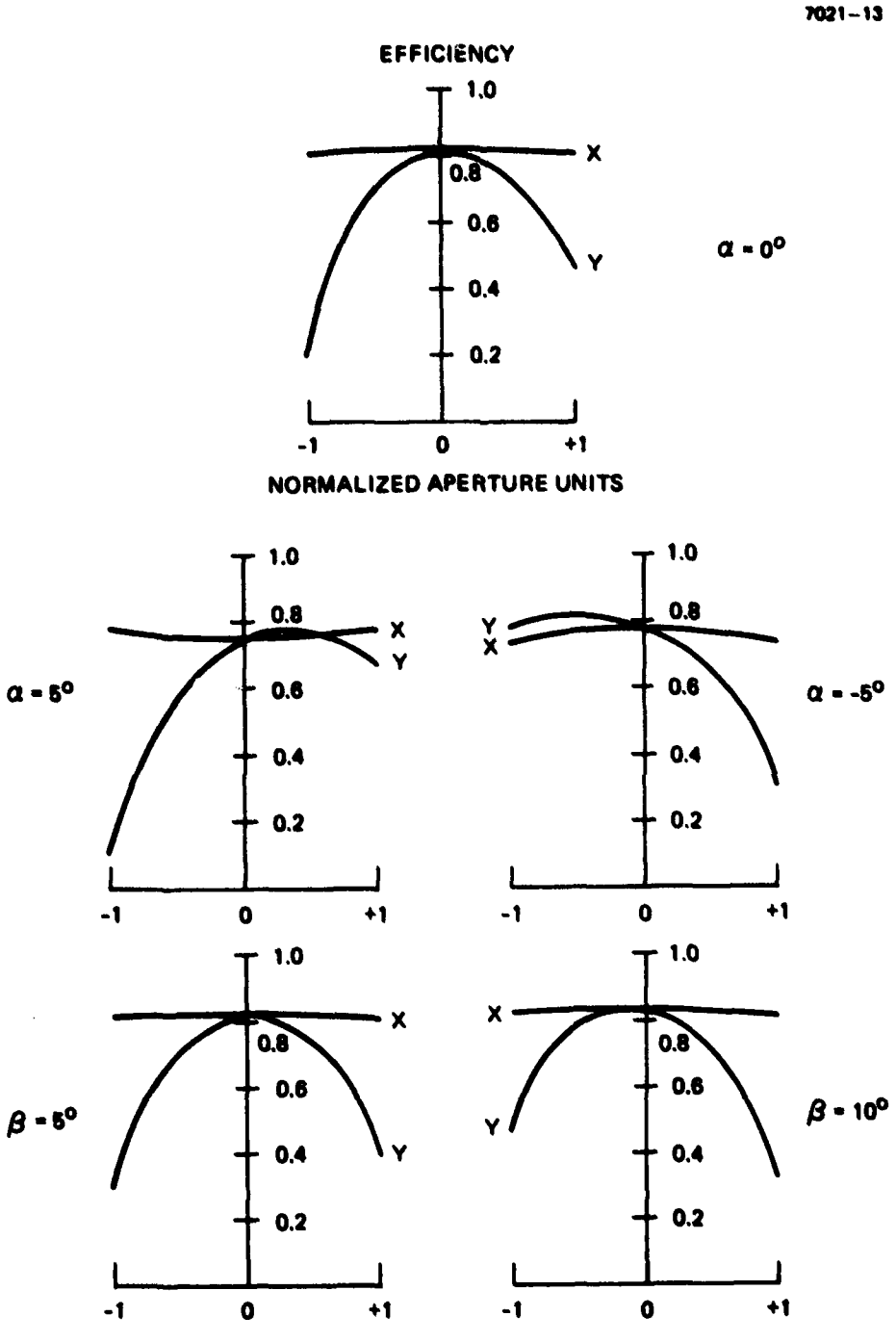

Figure 5. Variation in diffraction efficiency across the pupil for various field angles.

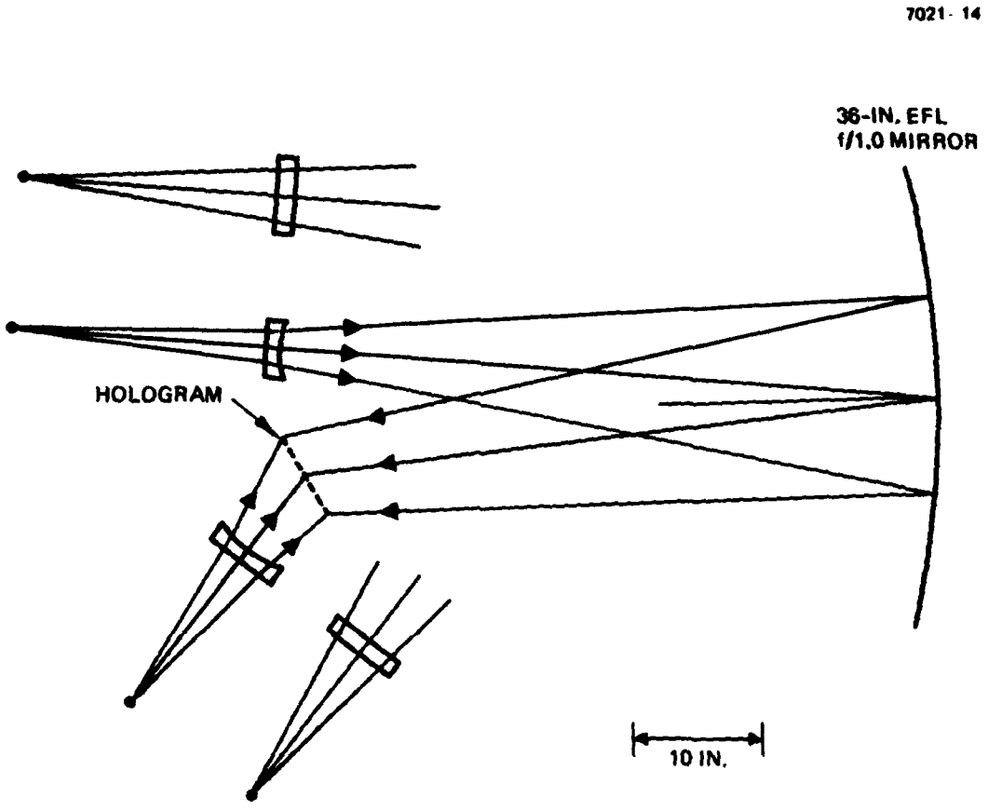

Figure 6. Construction beams for hologram in Phase 4 HHUD.

3. Relay Lens Design

Table 1 compares the Phase 3 and Phase 4 relay lens requirements. Because of the decrease in hologram focal length, the relay lens must work over a much larger FOV. Some work was done on the five-element triplet design (used in Phase 3) to determine its usefulness, but it could not image effectively over the larger FOV. A new relay lens — a five-element asymmetric lens — was chosen to meet the new requirements (see Figure 7).

B. HHUD PERFORMANCE

The performance of the Phase 4 HHUD is discussed in this section. The geometrical aberration curves are shown in Figure 8, and this data is summarized in Table 2 in terms of binocular disparity and collimation error.

The geometrical aberration curves were generated by tracing horizontal fans of rays at three positions in the pupil (Y = 1 in., Y = 0, Y = -1 in.) for various field angles. The fan of rays through the center of the pupil (Y = 0) covers the full 3.5-in. horizontal diameter. The fans at Y = 1 in. and Y = -1 in. cover only about 2.85 in. because of the particular shape of the pupil. Each of the rays in the fan was traced through the system, and its horizontal and vertical errors at the image source were calculated. These errors divided by the appropriate focal length (the system focal length is slightly different in the horizontal and vertical planes), which represent angular errors at the eye, are plotted versus the ray's entering position in the pupil. Imagining two eyes (separated by 2.4 in.) placed anywhere along the fan, the average of the vertical errors (the $\Delta\alpha$'s) is the vertical accuracy error and the difference is the vertical binocular disparity. Similar equations hold for horizontal errors (the $\Delta\beta$'s). The maximum of these errors is summarized in Table 2. Typically, they are in the 2 to 5 mrad region. As was the case in Phase 3 design, the largest errors occur at the larger field angles and at the edges of the pupil.

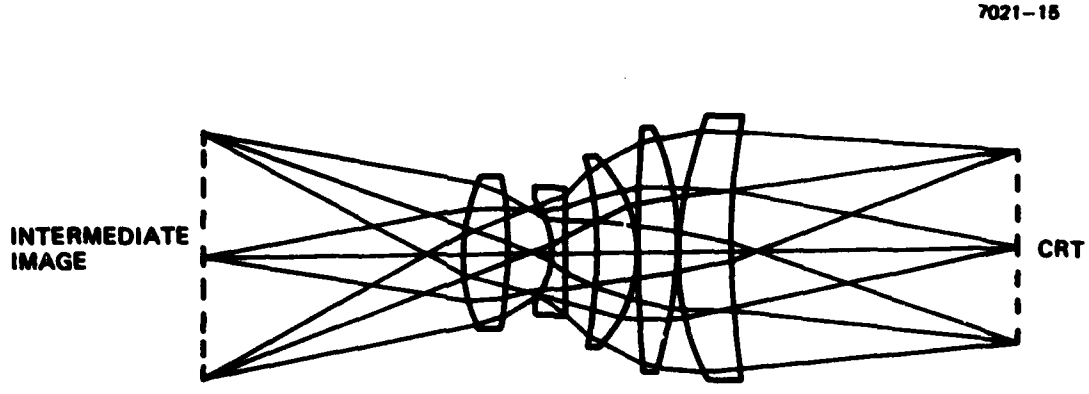

Figure 7. Preliminary design of five-element asymmetric relay lens.

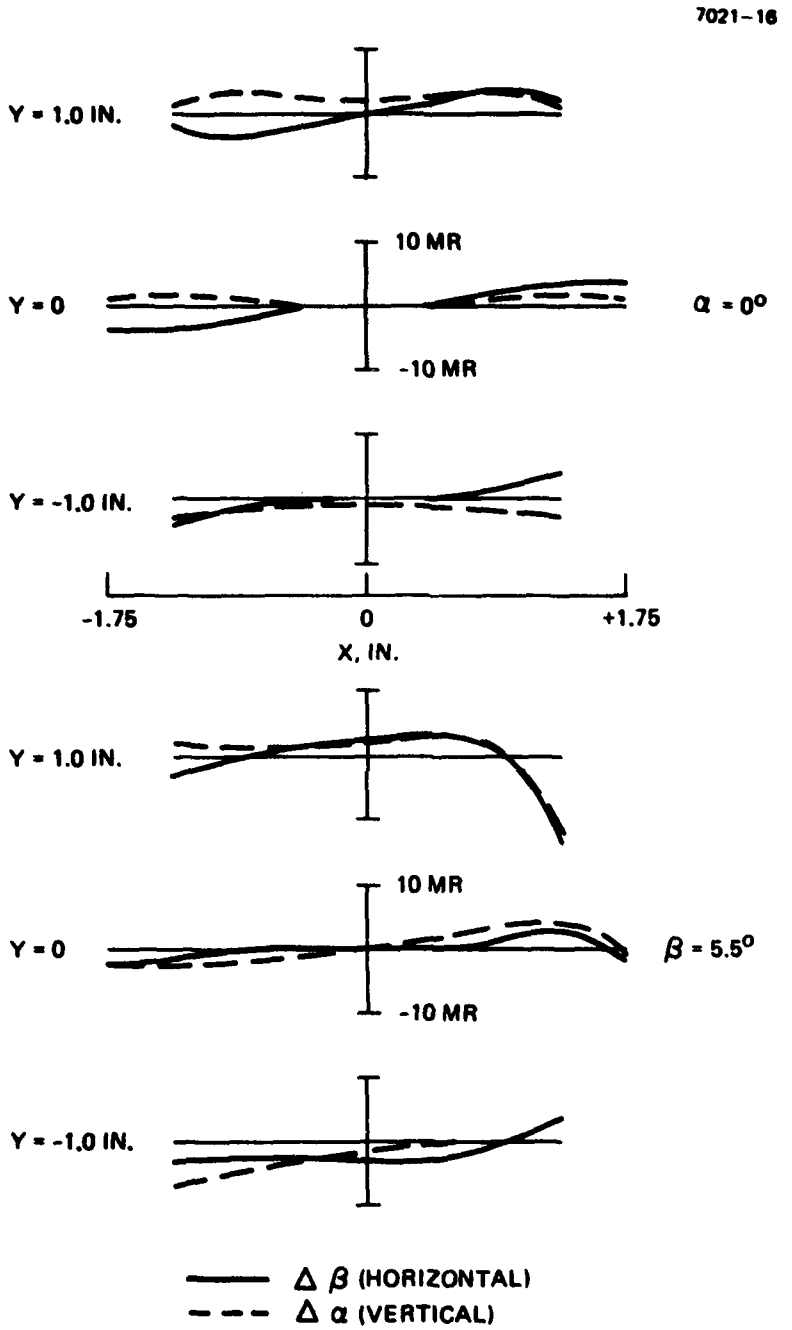

Figure 8. Geometrical aberrations of Phase 4 HHUD.

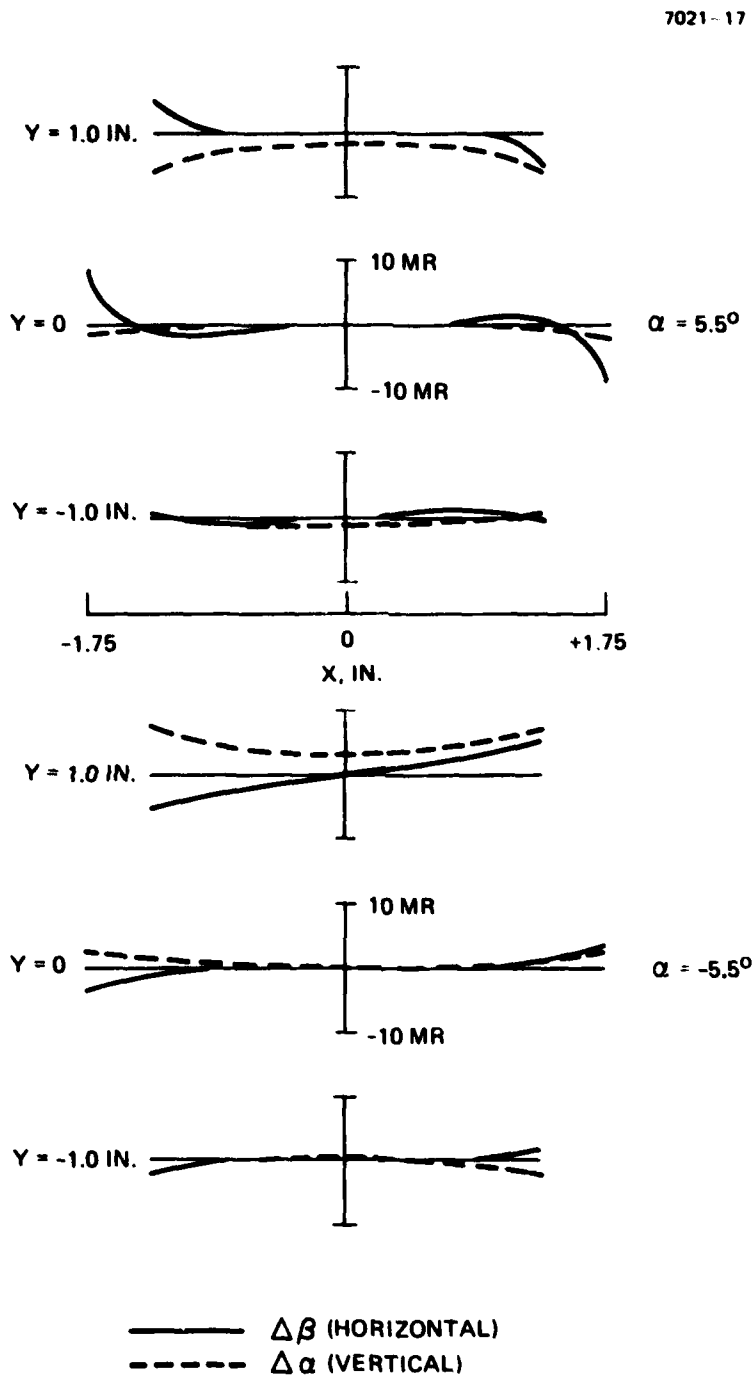

Figure 8. Continued.

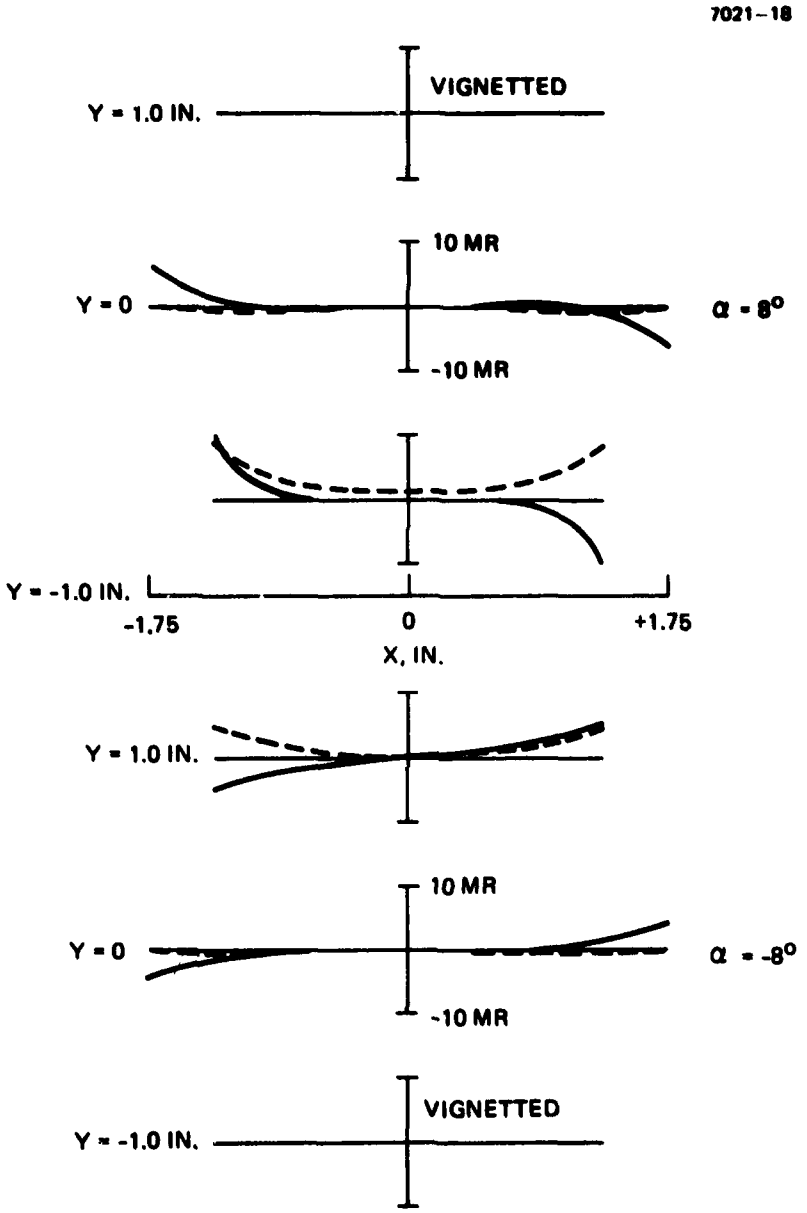

Figure 8. Continued.

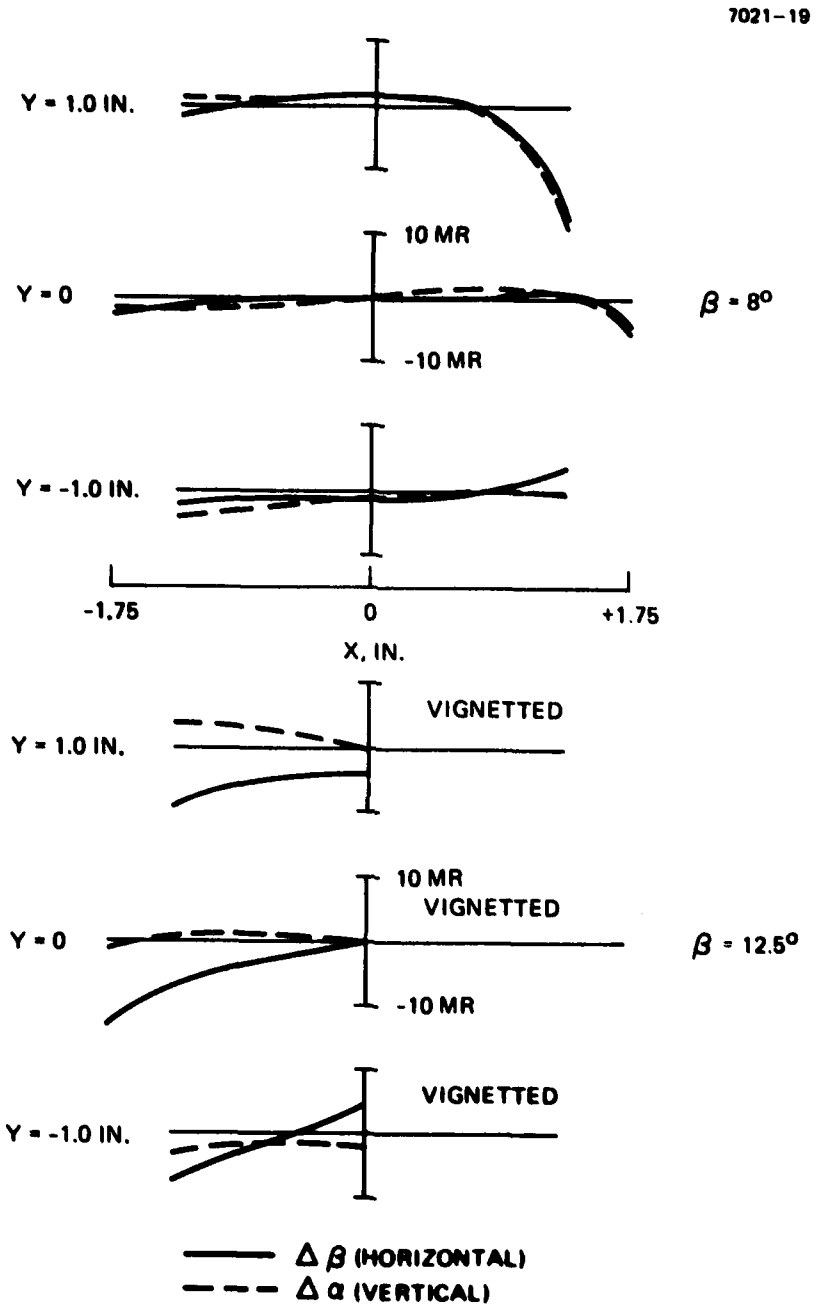

Figure 8. Continued.

C. RELAY-LESS HHUD

During Phase 4 we also investigated the functions of the relay lens in the operation of the HHUD and what performance is likely from a holographic display system in which a relay lens is not used or in which a holographic relay lens is used. The two major functions of the relay lens are

- To transfer a magnified image of the source (e.g., CRT) to the focal plane of the holographic lens and thereby allow a larger FOV for a given source size.
- To balance the aberrations present in the holographic lens by varying parameters during the system optimization.

The consequences of using a single flat-plate hologram without a relay lens are clear from the trade-off studies of Phase 3. Short focal length holograms (which are difficult to package in a cockpit) offer larger FOVs for a given CRT size; however, because of image tilt disparity, differing field curvatures, and large coma, they perform poorly. Longer focal lengths mean smaller FOVs but somewhat better performance. Even the best compromise offers only moderate FOVs and moderate performance.

D. HOLOGRAPHIC RELAY LENS

The limited usefulness of a relayless HHUD has direct bearing on the prospects of making a holographic relay lens. A holographic lens, for all its unique properties, has some of the limitations of its refractive or reflective counterpart. It is a single lens element and, as such, has limited image quality, depending on its speed, FOV, conjugates, etc. A multi-element refractive relay lens can achieve better image quality over a larger FOV and at higher speeds than can a single lens. If the holographic lens is viewed as a complex grating or interference filter, then in theory one can envision multiple holograms or multiple layers analogous to a multi-lens system, but the technical and material problems are very great.

A display that uses a relay lens has a real aperture stop imaged as the exit pupil. If the viewer's eye is within this exit pupil, he will see the entire FOV, with little head motion required. Outside of this exit pupil, he will not see the display. In a relayless display, since there is no aperture stop imaged as the exit pupil, the hologram becomes the limiting aperture. Greater head motion is required, and all parts of the FOV may not be visible simultaneously. In a HUD using a holographic combiner, the size of the exit pupil will be largely determined by diffraction efficiency, which is directly related to construction geometry.

To illustrate the points made in this section, a relayless display was designed. The resulting HHUD is shown in Figure 9. The display uses two flat-plate reflective holograms of nearly equal power and a wedge-like cylindrical field lens. The system focal length is determined by the individual hologram focal lengths and their separation, expressed by the equation:

$$1/f = 1/f_a + 1/f_b = d/f_a f_b \quad .$$

where d = distance separating the two holograms.

The optical characteristics of the display are summarized in Table 3. The second hologram is not performing any relay lens functions. By splitting the system power between two holographic elements, a decrease in aberrations was achieved. In the limit as one of the hologram focal lengths becomes large, the system becomes a single 14.2 in. focal length flat-plate hologram much like those in the Phase 3 trade-offs.

The prism/field lens serves to decrease the image surface tilt, which otherwise would cause the CRT source to extend beyond the available space. This function could also be performed by a fiber optics bundle. The location of the construction sources are shown in Figure 10.

The geometrical aberration curves for this design are given in Figure 11. Coma dominates the aberrations and results in the accuracy errors tabulated in Table 4. Because the system uses two holograms, the diffraction efficiency will be the product of the efficiencies at each hologram. If the peak efficiency for each hologram is 84%, then the

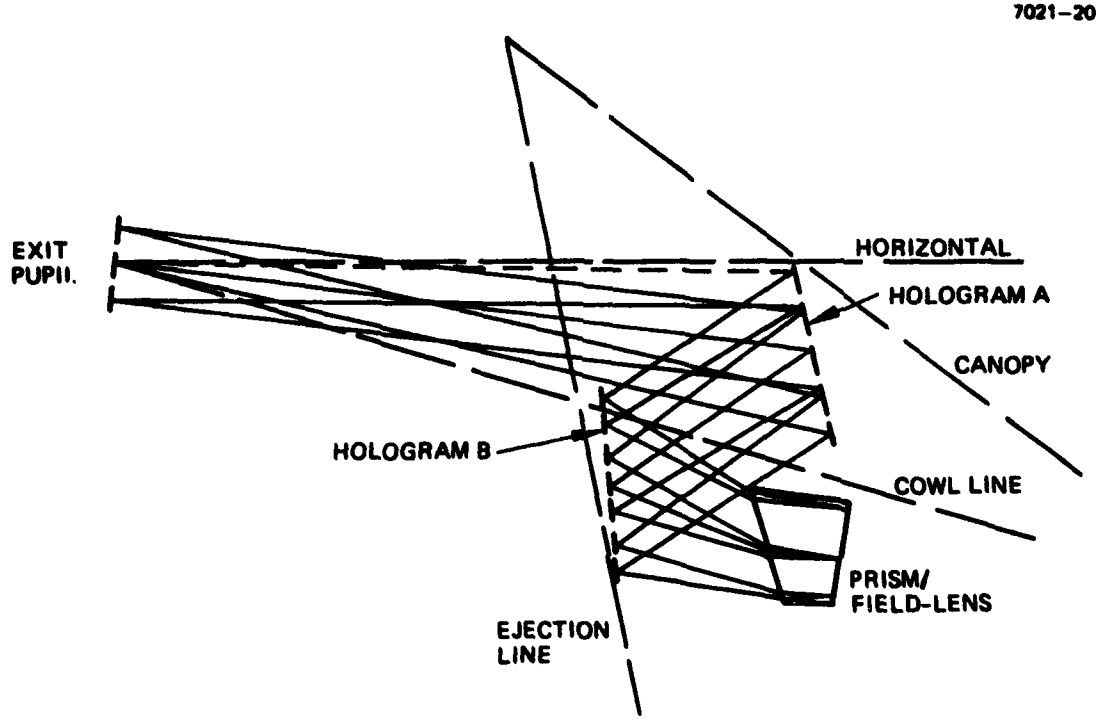

Figure 9. Vertical section of two-hologram relayless HHUD.

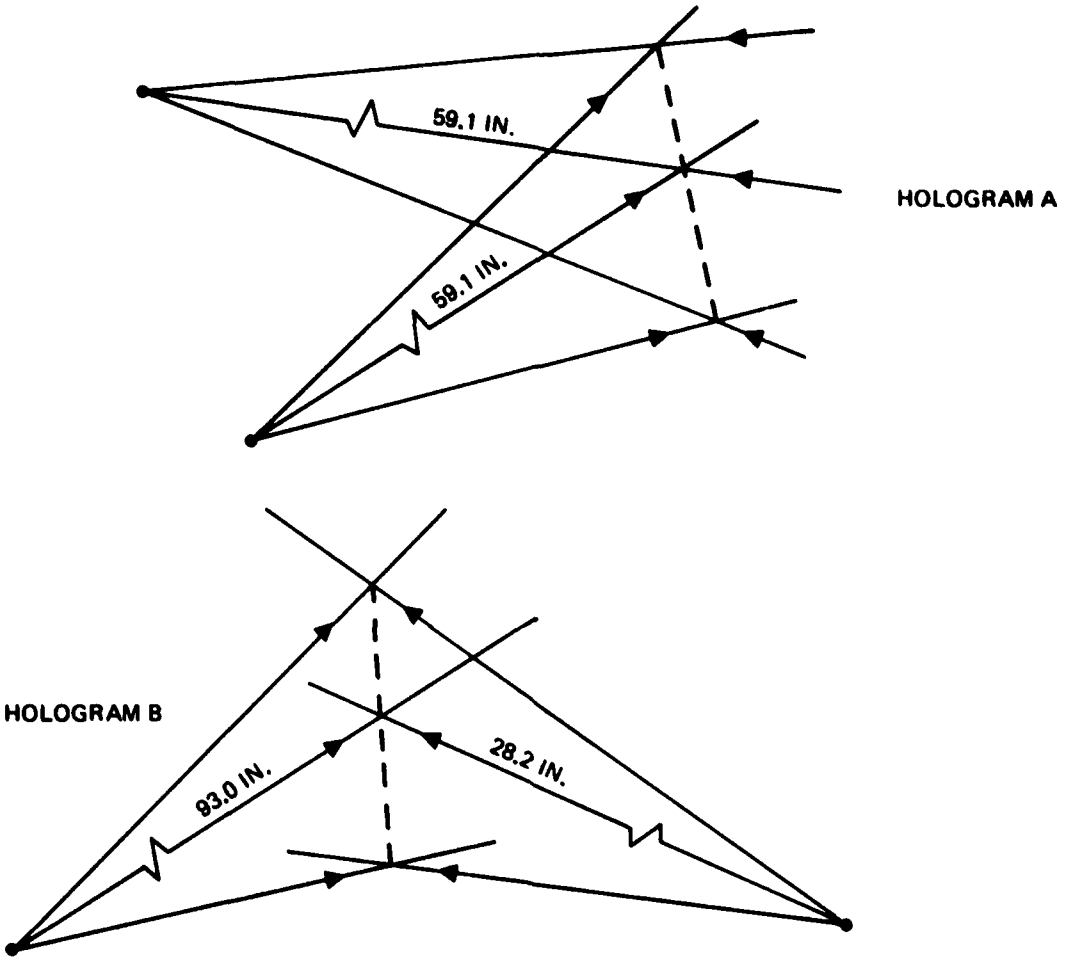

Figure 10. Location of construction sources for both hologram in the two-hologram relayless HHUD.

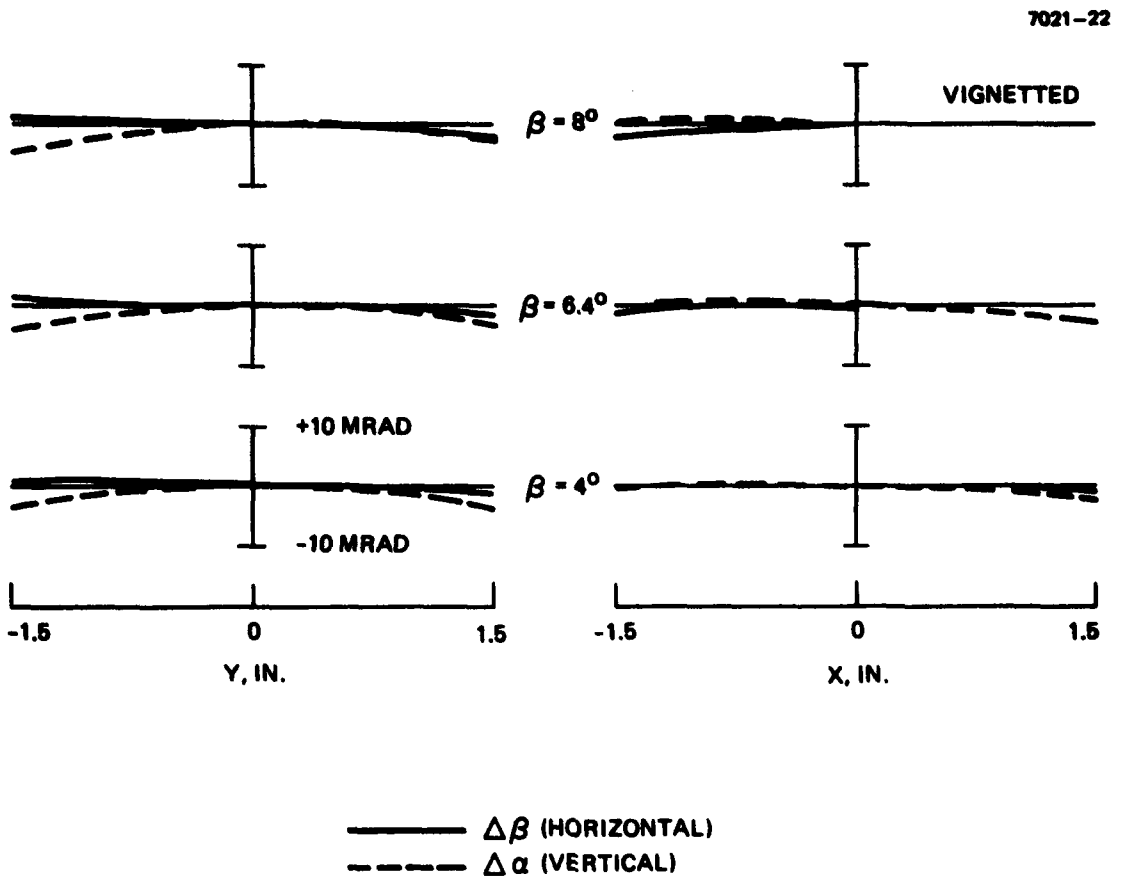

Figure 11. Geometrical aberrations of two-hologram relayless HHUD.

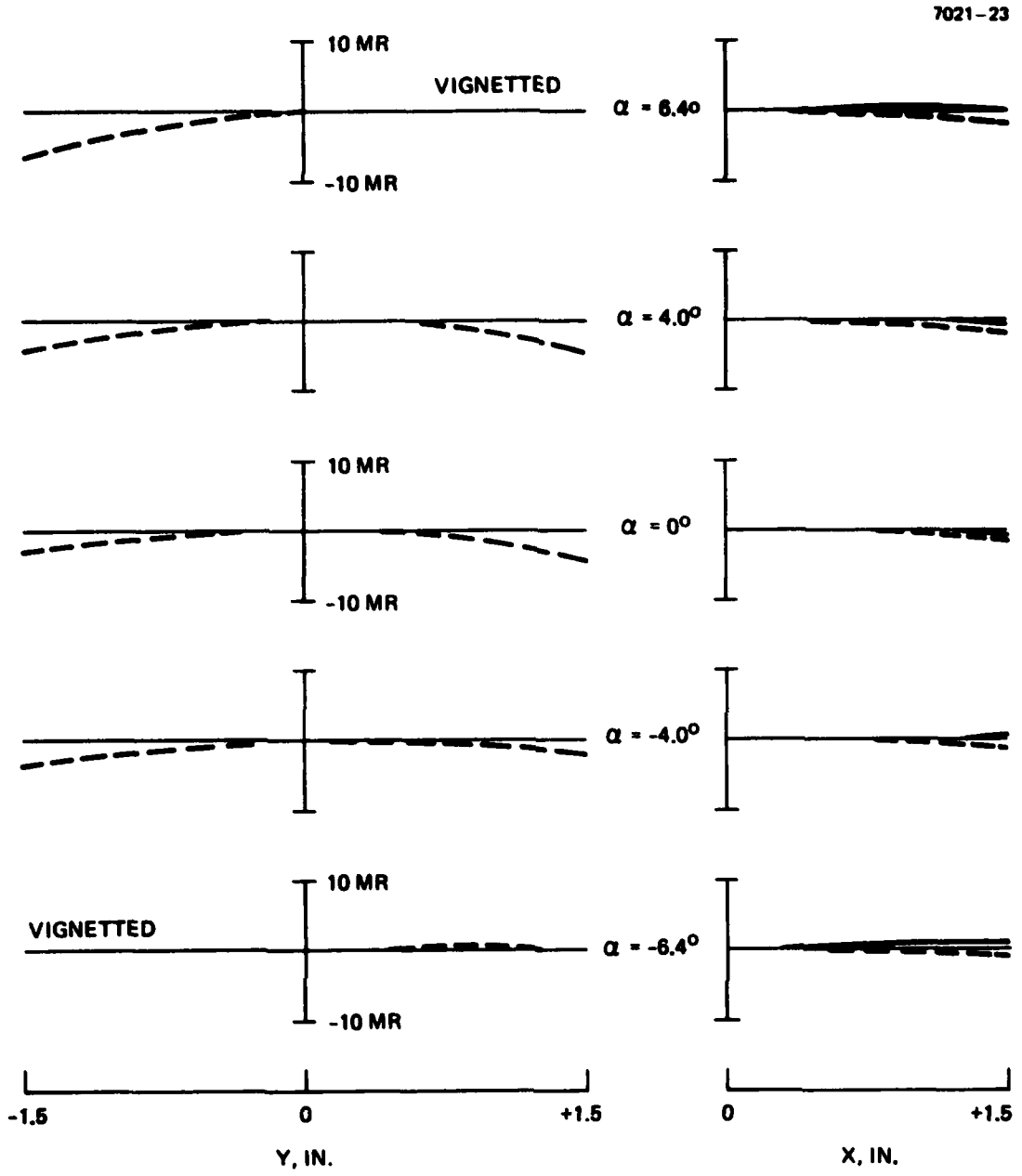

Figure 11. Continued.

Table 3. Optical Characteristics of Two-Hologram Relayless HHUD.

FOV, deg.	16 horizontal x 12.8 vertical
Exit pupil size, in.	3 (circular)
System focal length, in.	14.2
Assumed CRT size, in.	4
Eye relief, in.	29
Hologram A	
Focal length, in.	28.0
Bend angle, deg.	40
Hologram B	
Focal length, in.	16.4
Bend angle, deg.	56

6029

Table 4. Performance Summary of Two-Hologram Relayless HHUD.

Field Angle	Accuracy Error,[a] mrad	Binocular Disparity,[a] mrad	
		Horizontal	Vertical
$\alpha = 0°$	4	1	0
$\alpha = 4.0°$	5	2	0
$\alpha = -4.0°$	3	1	0
$\beta = 4.0°$	3.5	1	2
$\alpha = 6.4°$	7	1	0
$\alpha = -6.4°$	1	2	0
$\beta = 6.4°$	3	1	2.5
$\beta = 8.0°$	4.5[b]	-	-

[a]Errors quoted are maxima.
[b]Monocular.

6029

maximum efficiency for the system is about 70%. The efficiency across the pupil for several field points is shown in Figure 12.

In summary, a relayless HHUD, particularly one using a flat-plate hologram, will be limited to a moderate FOV and will have only moderate performance. Uncorrected coma results in accuracy errors that can be large.

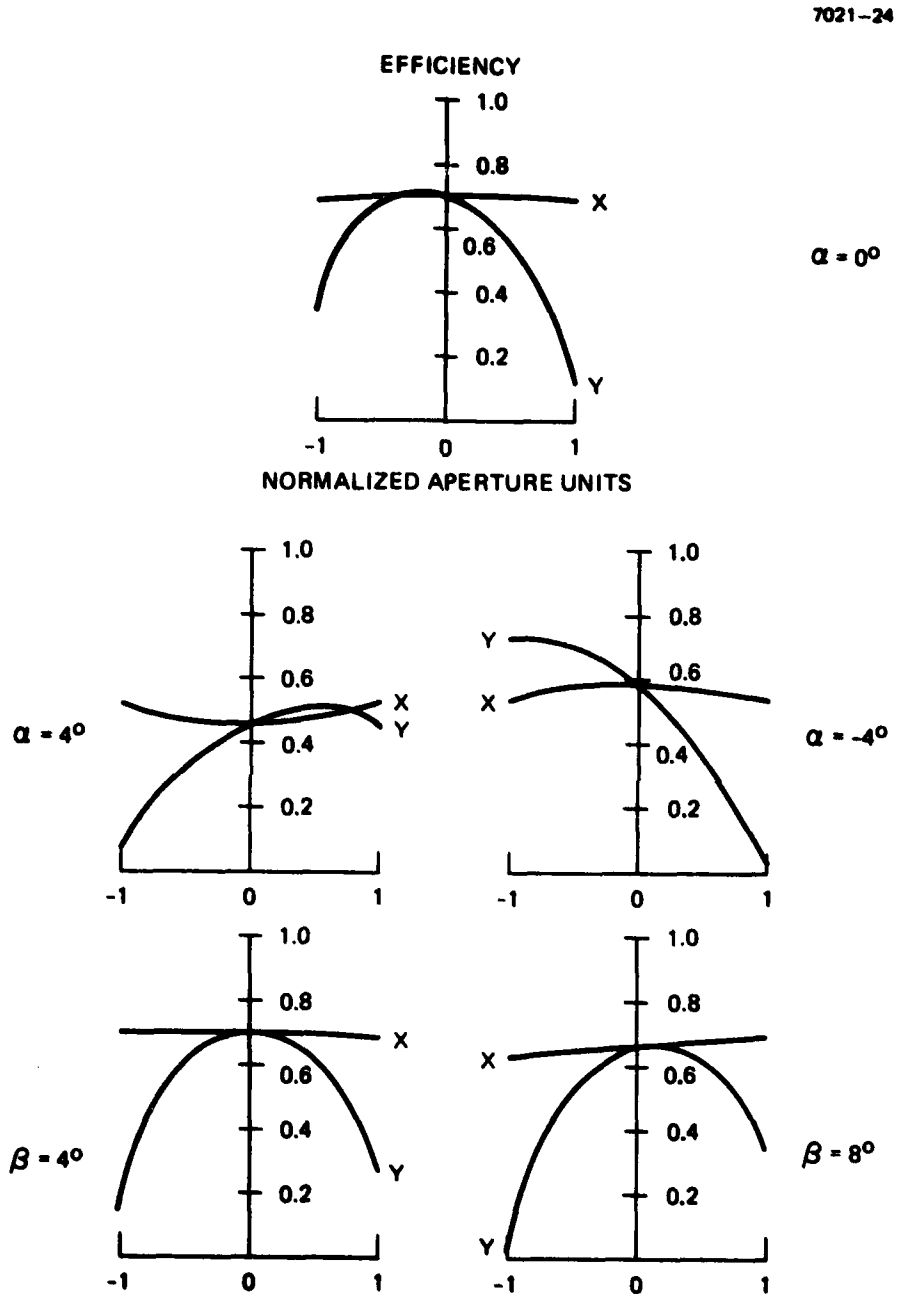

Figure 12. Variation in diffraction efficiency of the two-hologram relayless HHUD across the pupil, for various field angles.

SECTION 3

HHUD (DEMONSTRATOR) DESIGN AND SPECIFICATION

Phase 4 provided for fabrication of a hologram that could be used in the AIDS demonstrator to illustrate the properties and operation of a reflective holographic lens. What was needed was a moderate FOV system that could be viewed with two eyes and was simple, but not necessarily one that conformed to the rigid geometry requirements of a fighter cockpit.

A. SYSTEM DESIGN AND SPECIFICATION

The relayless system is shown along with the AIDS cockpit lines in Figure 13. The holographic lens acts as an eyepiece to give the viewer a collimated image of the information on the CRT face. Table 5 lists the optical characteristics of the display. The hologram focal length chosen was short enough to give a moderate FOV (for a given CRT size) and yet long enough to minimize aberrations and allow the CRT to clear the user's head. Because of the absence of a relay lens, many of the considerations covered in Section 2.C and 2.D are applicable here, especially those concerning the lack of an imaged exit pupil. The construction geometry for this hologram is pictured in Figure 14.

B. ABERRATIONS AND EFFICIENCY

The geometrical aberration curves for this hologram are shown in Figure 15. As expected, coma is the dominant aberration and is fairly consistent across the FOV. Variation in diffraction efficiency across the pupil for various field angles is shown in Figure 16.

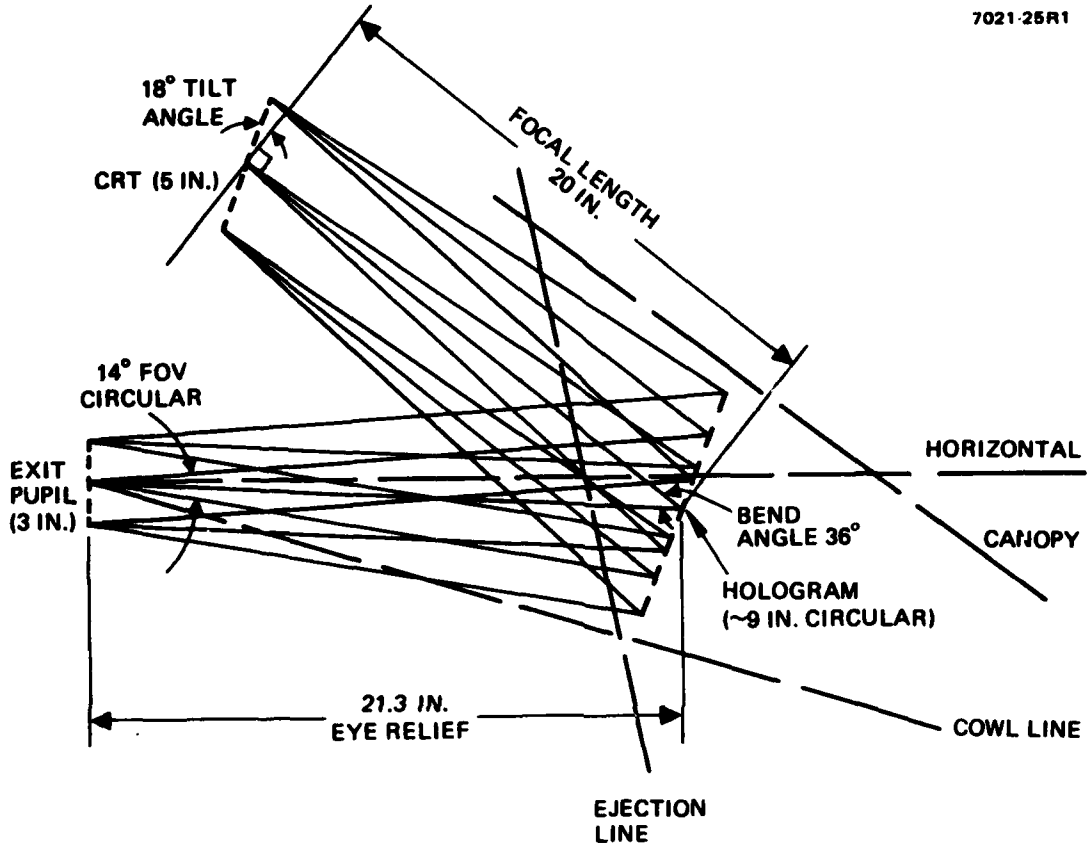

Figure 13. Holographic lens for fabrication shown in AIDS demonstrator cockpit.

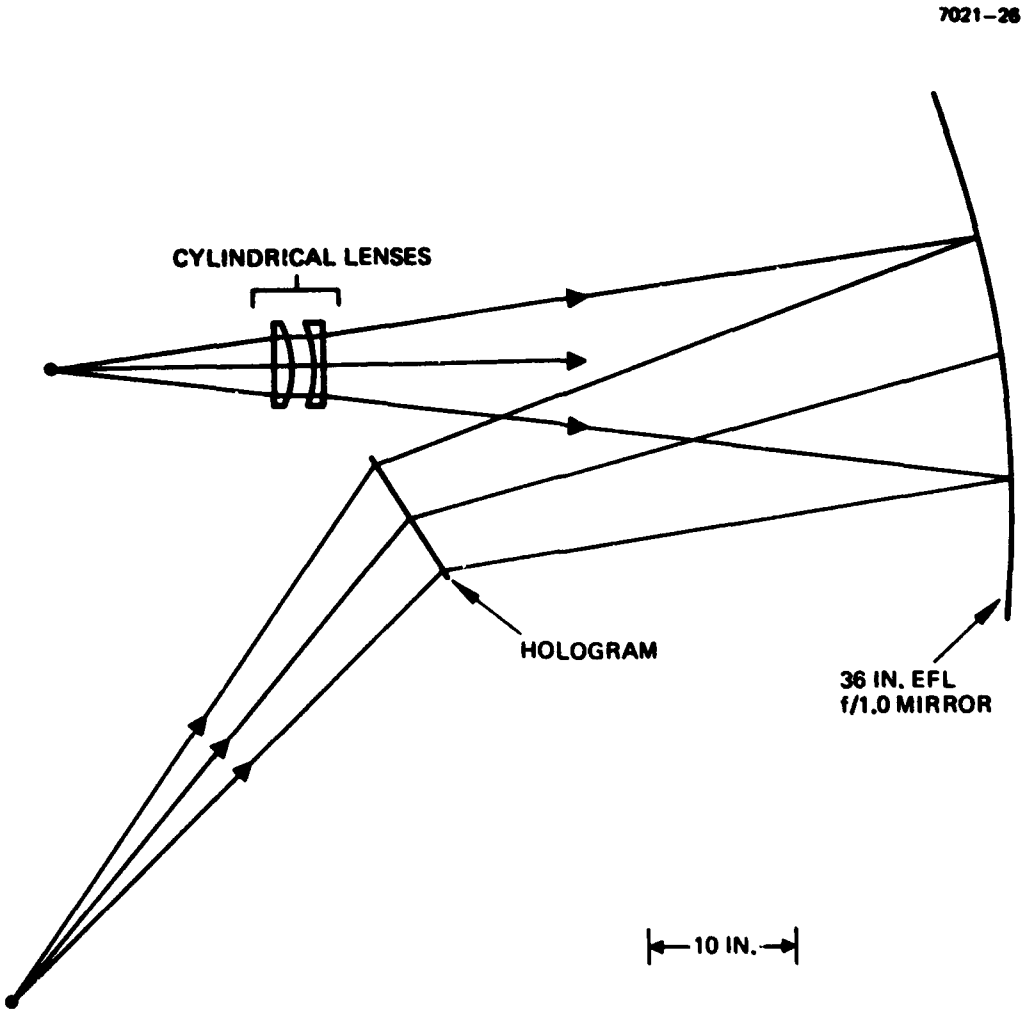

Figure 14. Construction geometry for the demonstration hologram.

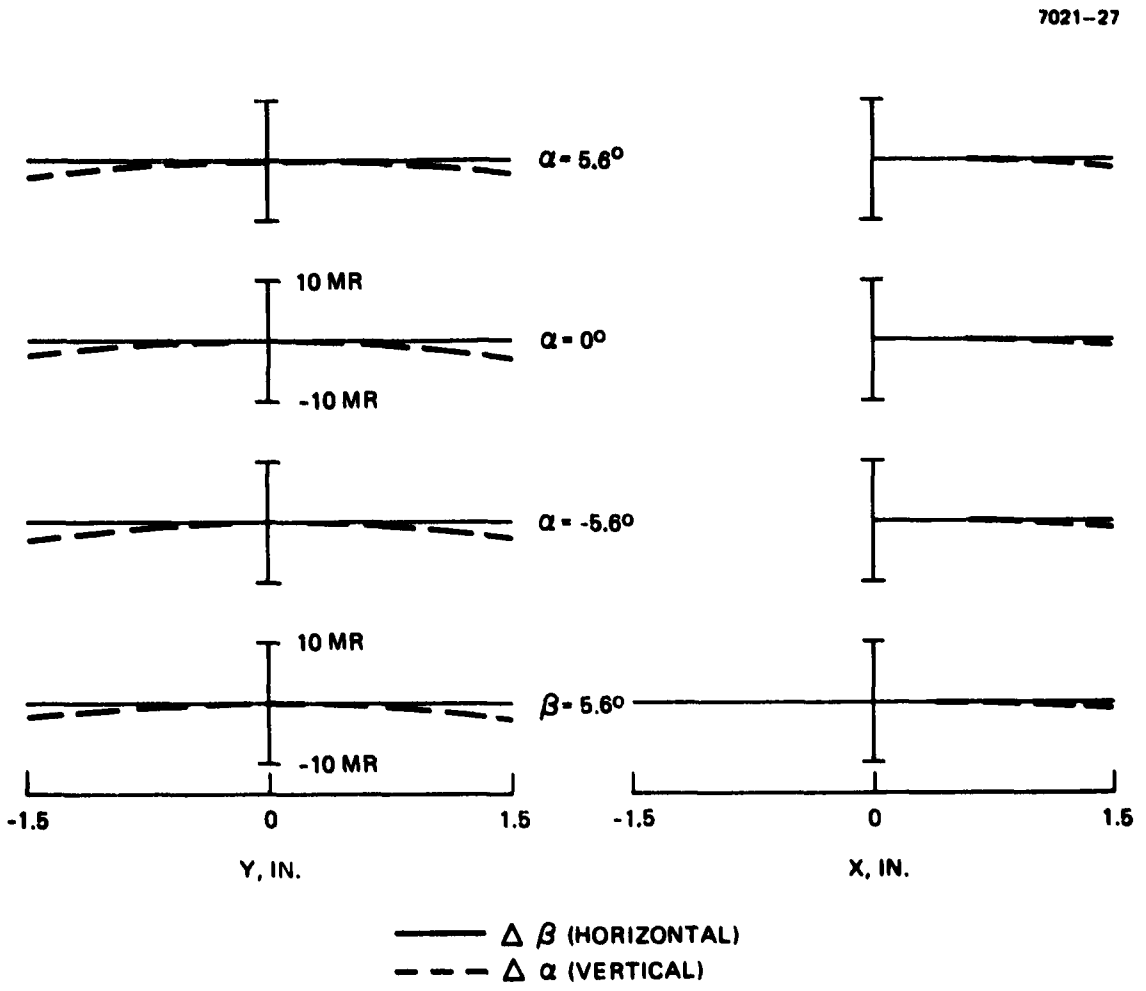

Figure 15. Geometrical aberrations of holographic lens for fabrication.

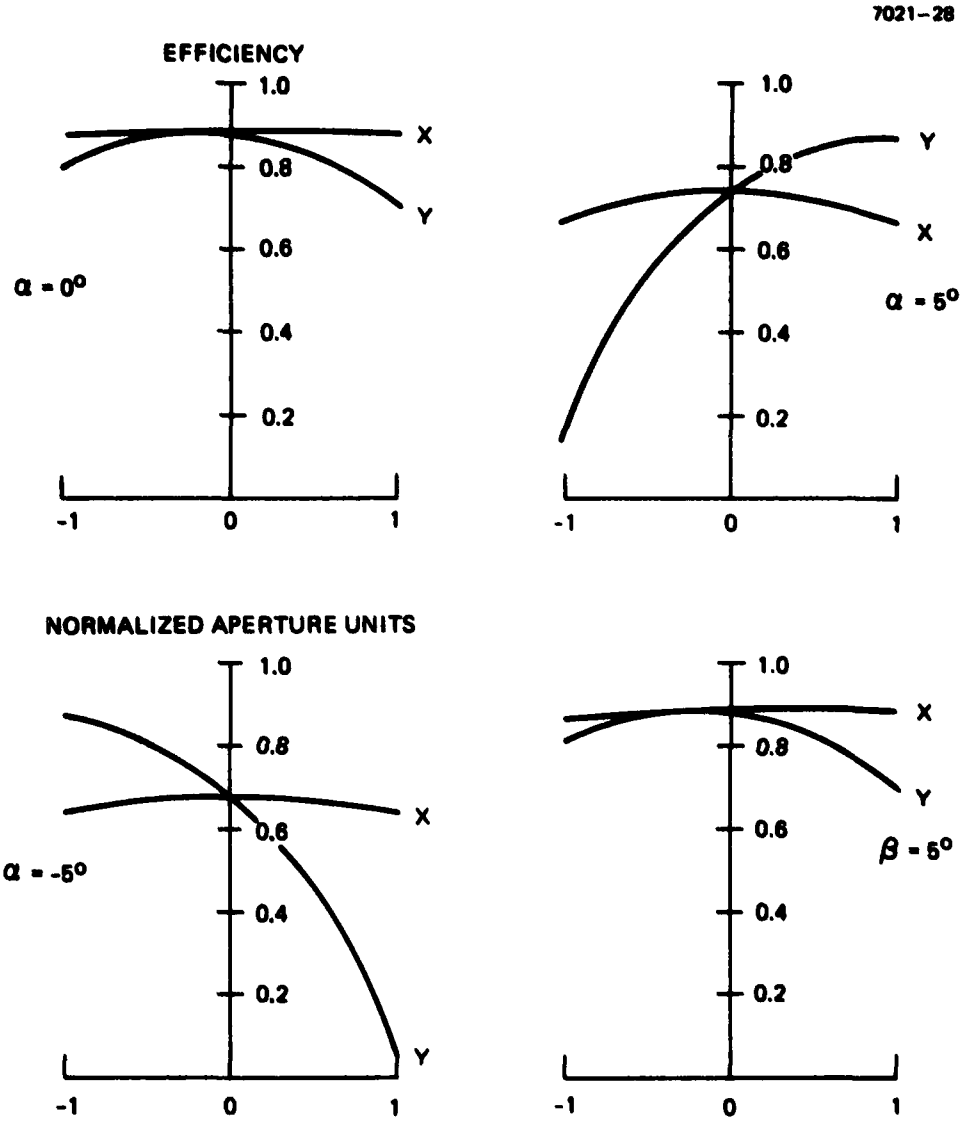

Figure 16. Variation in diffraction efficiency across the pupil for various field angles in demonstrating hologram for fabrication.

Table 5. Optical Characteristics of Holographic Lens for Fabrication.

FOV, deg.	14 (circular)
Exit pupil size, in.	3 (circular)
Focal length, in.	20
Assumed CRT size, in.	5
Eye relief, in.	21.3
Bend angle, deg.	36
Hologram size, in.	∿9 (circular)
CRT tilt, deg.	18
Maximum accuracy error, mrad	∿3
Average disparity error, mrad	∿1.5

6029

SECTION 4

REFLECTION HOLOGRAM FABRICATION AND TEST

A holographic lens was fabricated in accordance with the AIDS demonstrator design and specifications (Section 3). The 36° off-axis reflection hologram lens was recorded in dichromated gelatin for use with a P-43 phosphor CRT display (5430 Å wavelength). The hologram aperture is ≈8 in. in diameter covering ∿14° circular FOV from any point within a 3 in. circular pupil at an eye relief of 21.3 in.

A. RECORDING MATERIAL AND MATERIAL PROCESSING

Selection of a photosensitive material for a holographic lens application requires carefully considering the criteria imposed by the optical system design. For the HUD application, the necessary qualities of permanence, high resolution, environmental endurance, good optical quality, and freedom from scattering noise led to the selection of dichromated gelatin. During Phase I, we concluded that when the added requirements of large index modulation and diffraction efficiency are considered, only dye-sensitized dichromated gelatin (DSDCG) and dichromated gelatin (DCG) have the necessary properties.[2] This selection of the holographic recording material is still valid for the HHUD application.

During Phase 4, it was decided to change the operational color of the HUD from red to green. Correspondingly, the spectral sensitivity of the hologram recording material had to be re-evaluated, and DCG without dye sensitization was selected. The optimization techniques developed earlier from DSDCG were still applicable to DCG.

1. Dichromated Gelatin

DCG has been a popular hologram recording material since its practicability was demonstrated by Shankoff[5] in 1968. DCG materials display considerable variability stemming from the complex biochemical structure of gelatin and the mechanical nature of the recording process.

A primary goal in materials preparation was to improve reproducibility through exact process control while maintaining holographic characteristics commensurate with the program goals.

We adopted the materials preparation procedures developed for DSDCG during Phase 1. (Reference 2.) The postulated photochemical mechanisms for image formation for the DCG and DSDCG systems are very similar, as shown in Figure 17. The major difference is in the energy-absorbing species for the long and short wavelength photons. In a related IR&D program, we had adapted these methods to apply to the new HUD operational wavelength and the recording geometry of the reflection type.

In a hologram, the spacing of the fringe lines partially determines the wavelength at which the hologram will diffract most efficiently. For reflection holograms, the proper fringe spacing is more difficult to maintain since the fringes do not generally intersect the substrate surface as do transmission holograms.

The desired playback wavelength for the final combiner material is 543 nm, the operational spectral band of the P-43 CRT phosphor. The hologram, however, is constructed at the shorter wavelength of 514.5 nm. As a consequence, the Bragg plane spacing in the hologram after light exposure is closer than desired. The increase in the fringe spacing is obtained as part of the available DCG development process. After exposure, the hologram is swollen with water to remove the unreacted dichromate, and the film is expanded to where the fringe spacing is larger than that desired. In the second development step, the water is removed by rapid dehydration, and the hologram is dried to shrink the spacing down to have a wavelength equal to the desired 543 nm.

B. EXPOSURE AND TEST

Reflection holographic lenses for the AIDS demonstrator were successfully fabricated with 75% efficiency at the operating wavelength of 5430 Å. Exposure times of 30 min. were required to expose the 8 in. x 10 in. holographic emulsion with 300 mJ/cm^2 of energy.

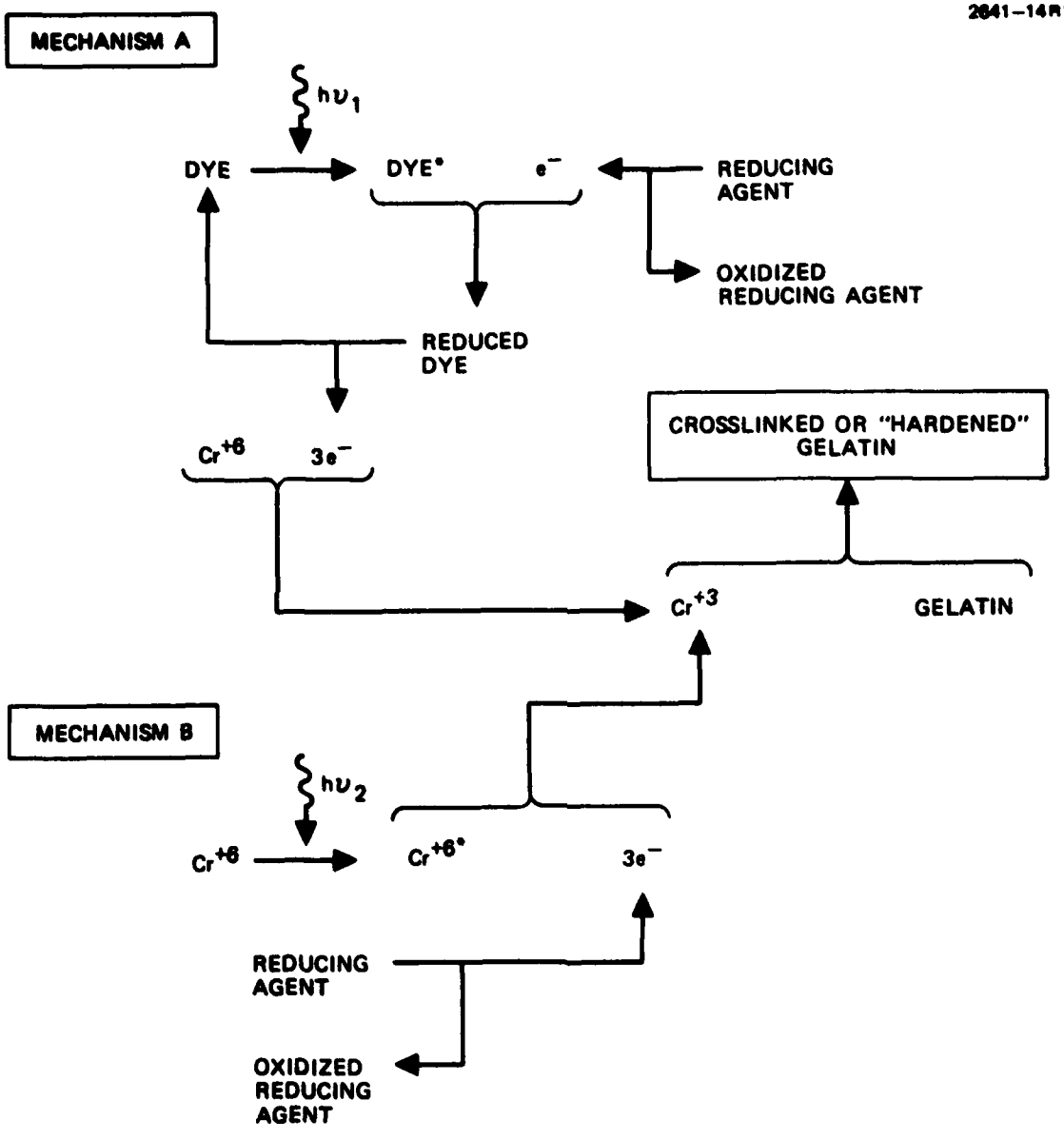

Figure 17. Postulated mechanisms for image formation is DSOCG (mechanism A) and DCG (mechanism B).

1. Laser, Optics, and Mounts

The decision to change the operational color of the head up display from red (6328 Å) to green (5430 Å) made the replacement of the krypton ion laser tube with an argon ion tube necessary to obtain high recording laser power at 5145 Å. An etalon was added for increased coherence length with single-frequency operation. Output power of the Spectra Physics Model 165-03 argon laser was 1400 mW in the single transverse TEM_{∞} mode. A 50% conversion efficiency of the etalon reduced the available output power to 700 mW of single frequency power at 5145 Å. Coherence length was measured using the laser test set up described in Reference 4. At a 180 cm path length difference, the fringe visibility was 0.80.

Major construction optics consisted of elements procured and used in Phases 2 and 3. Two cylindrical lenses (±8.170-in. radius of curvature) provided optimum compensation of off-axis aberration of the 36-in. diameter, 72-in. radius of curvature spherical mirror. Other optics consisted of spatial filters for beam spreading and dielectric mirrors for beam steering.

Where possible, the construction hardware designed and fabricated for use in previous programs was used to assemble the exposure system. To position mounts at locations where threaded inserts were not accessible in the granite table surface, mounts with gravity bases were designed and fabricated. A hologram plate holder was also designed and fabricated to provide stable support of the 8-in. x 10-in. emulsion plate during exposure.

2. Construction Beam Optical System

Construction beam optical system design of Section 3 is shown in Figure 18. This design was used to fabricate the reflection holographic lens for a relayless HHUD system for the AIDS demonstrator. The 36-in. diameter, 72-in. radius of curvature spherical mirror forms the converging beam. Aberrations caused by using the mirror off-axis were reduced by reducing the off-axis angle and improving the positioning of

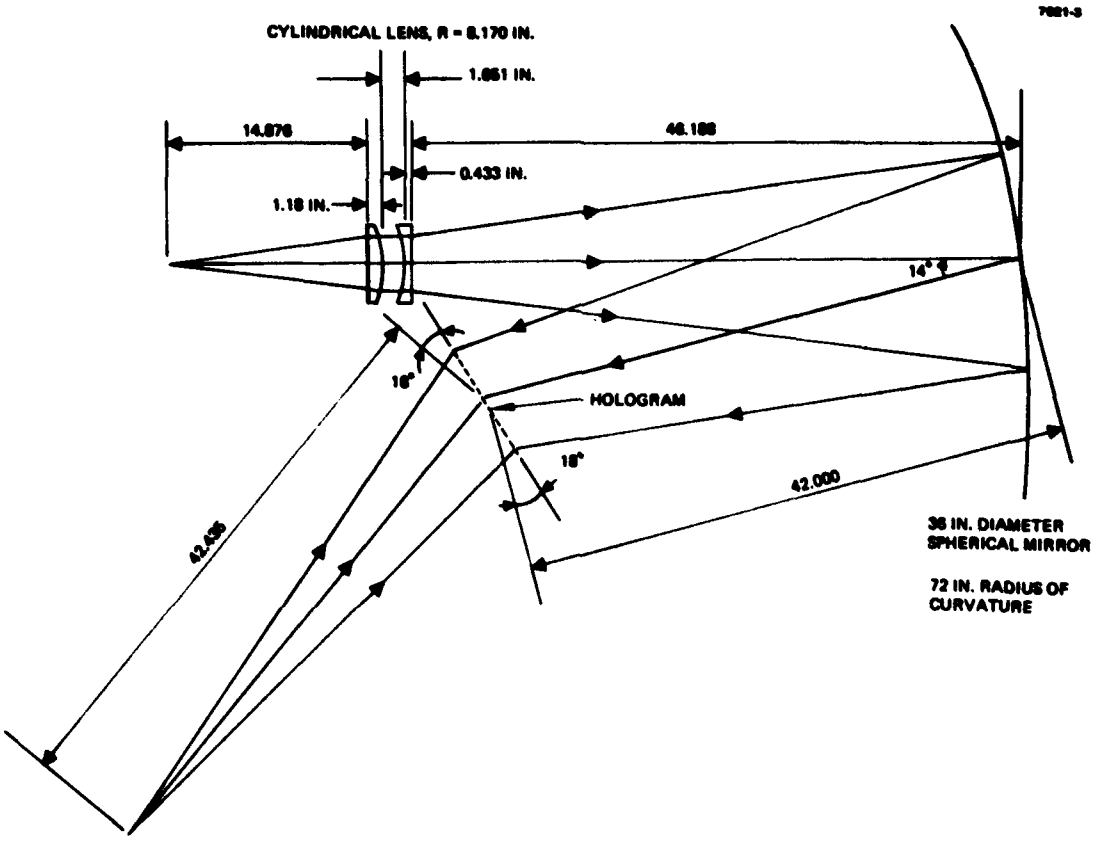

Figure 18. Construction beam optical system of 36° off-axis, symmetric reflection hologram-lens (Phase 4 fabrication hologram).

the cylindrical lenses. A diverging point source 42.44 in. from the hologram forms the other beam. The hologram exposure plane normal bisects the 36° off-axis angle between construction beams for this symmetric configuration.

Layout of the construction beam optical system on the 5 ft. by 10 ft. granite exposure table is shown in Figure 19 along with the fringe stabilization and monitoring systems. To keep all beam heights as low as possible for stability, the recording laser beam was separated into two levels. The lower level construction optics consist of small aperture mirrors, beam splitters, and a piezoelectric translator. It is used for path length matching to the center of the hologram exposure plane and to steer the laser beam to specified locations in the optical design. The laser beam is then directed up to the second level, 19.25 in. above the granite table where the construction beam optical system is assembled.

The assembled exposure system is pictured in Figure 20 within the acoustic enclosure for environmental stability. Low resonance air mounts supporting the granite table decoupled the exposure system from mechanical and building vibrations. Fringe stability of better than $\lambda/20$ was observed.

3. Stability-Control and Monitoring System

The holographic lens is a recording of the fringes formed by interference between the object and reference construction wavefronts. These interference fringes correspond to sinusoidally varying intensity planes. To record high contrast fringes accurately, instability caused by building and mechanical vibrations, unstable optical mounts, and acoustic and thermal disturbances must be minimized.

For the 36° off-axis symmetric reflection hologram, the spacing between interference peaks is 2.705×10^{-7} m/cycle ($d = \lambda/2 \sin \theta/2$, where θ is the included angle between construction beams). These interference fringes exist in space and are subject to the motion of the holographic emulsion and substrate as well as environmental disturbances.

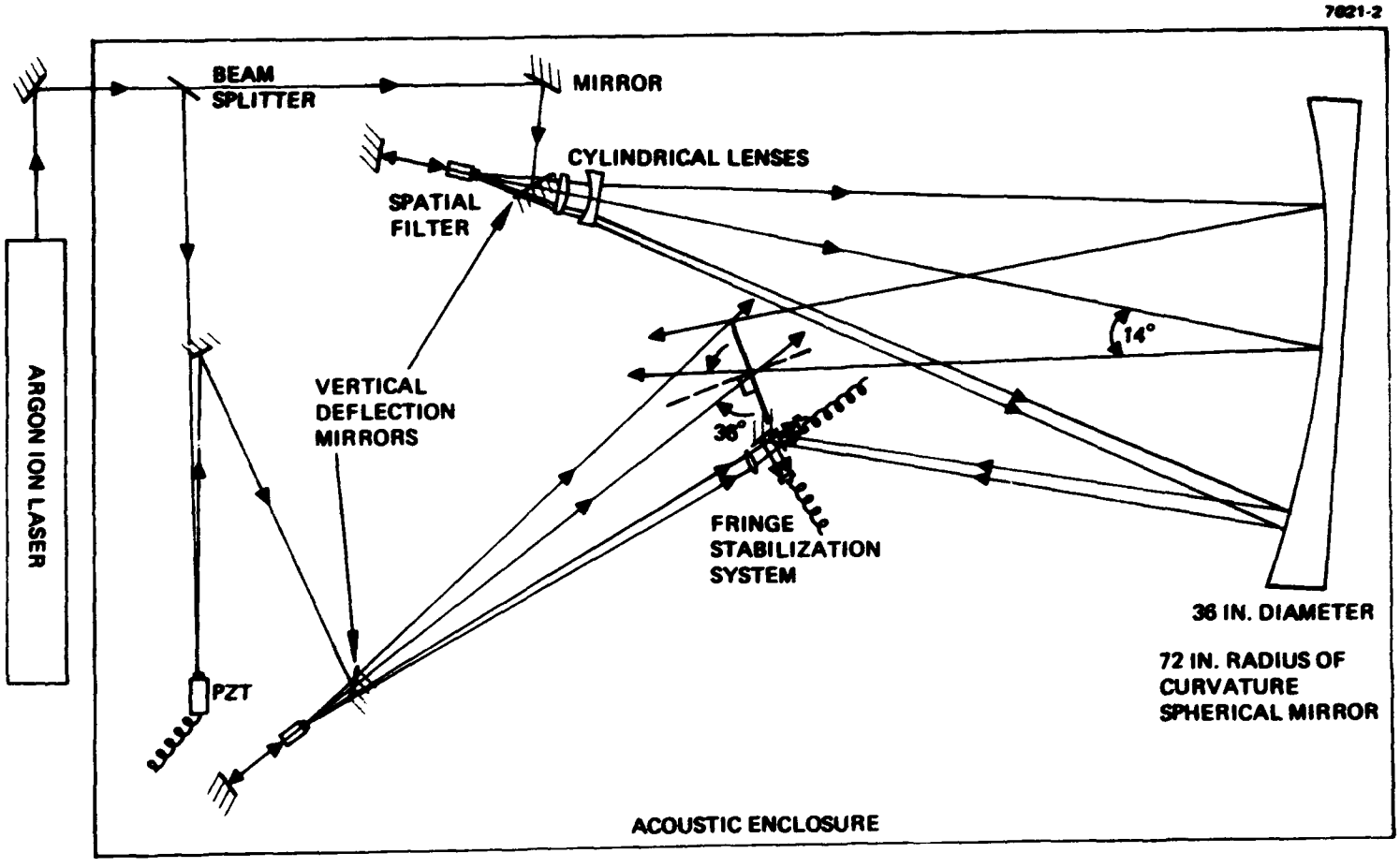

Figure 19. Layout of construction beam optical system on the 5 ft x 10 ft granite exposure table for 36° off-axis, symmetric reflection hologram.

Figure 20. Heads-up display reflection hologram lens recording system.

For reflection geometry where fringes lie parallel to the emulsion, motion perpendicular to the emulsion can also cause fringe blurring during an exposure. Therefore, stability of the substrate and holder must also be maintained to a fraction of the fringe spacing.

The required stability was achieved in the assembled recording system by an active fringe control system (Figure 21) to correct for instability caused by phase perturbation of the construction wavefronts. A small portion of the construction wavefronts are mapped onto each other at a small angle, which creates two identical, out of phase, low spatial frequency interference patterns. These detection fringes vary linearly with the phase of the recorded interference at the hologram lens. Inputs to feedback electronics are provided with photodiodes which monitor the intensity of the interference patterns. An error signal from the feedback electronics modulates a piezoelectric translator mirror in one leg of the construction beams to actively correct the phase. A closed-loop system locks the intensities of the detection interference at a reference level providing better than $\lambda/20$ fringe stability during the long exposure time required to record large aperture reflection holograms. This active fringe control system is discussed in detail in Reference 3.

4. Display Geometry

The display geometry for the 36° off-axis symmetric reflection hologram is shown in Figure 22. The CRT is located 20 in. from the hologram. The focal plane is defined with an 18° CRT tilt because of the field tilt of the vertical ray fans. The designed eye relief and exit pupil of the system are 21.3 in. and 3 in. circular. The vertical and horizontal FOVs of the display system are shown in Figure 23 for an 8 in. x 10 in. holographic lens aperture size.

We proposed two other alternate display geometries (Figures 24 and 25) that permit convenient location of the P-43 CRT source. Both alternates utilize a folding mirror to bend the source location away from the exit pupil.

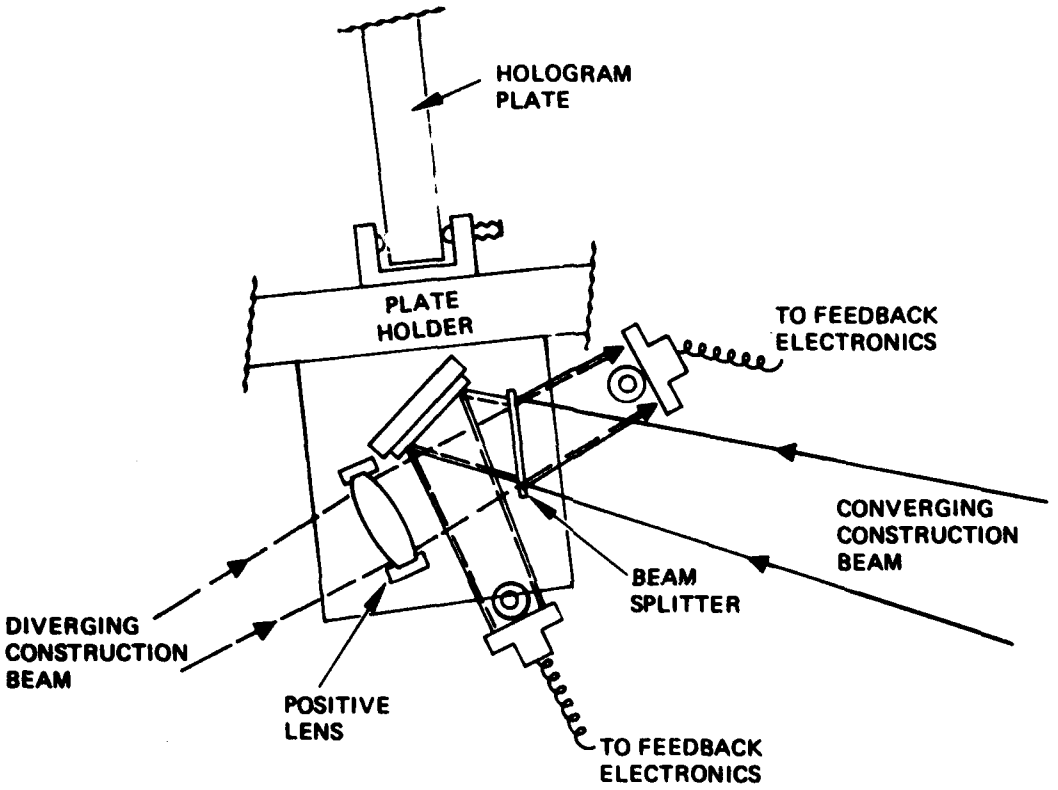

Figure 21. Fringe control interferometer maps the construction wavelength to form two identical, out-of-phase low-spatial-frequency interference patterns for fringe stability control.

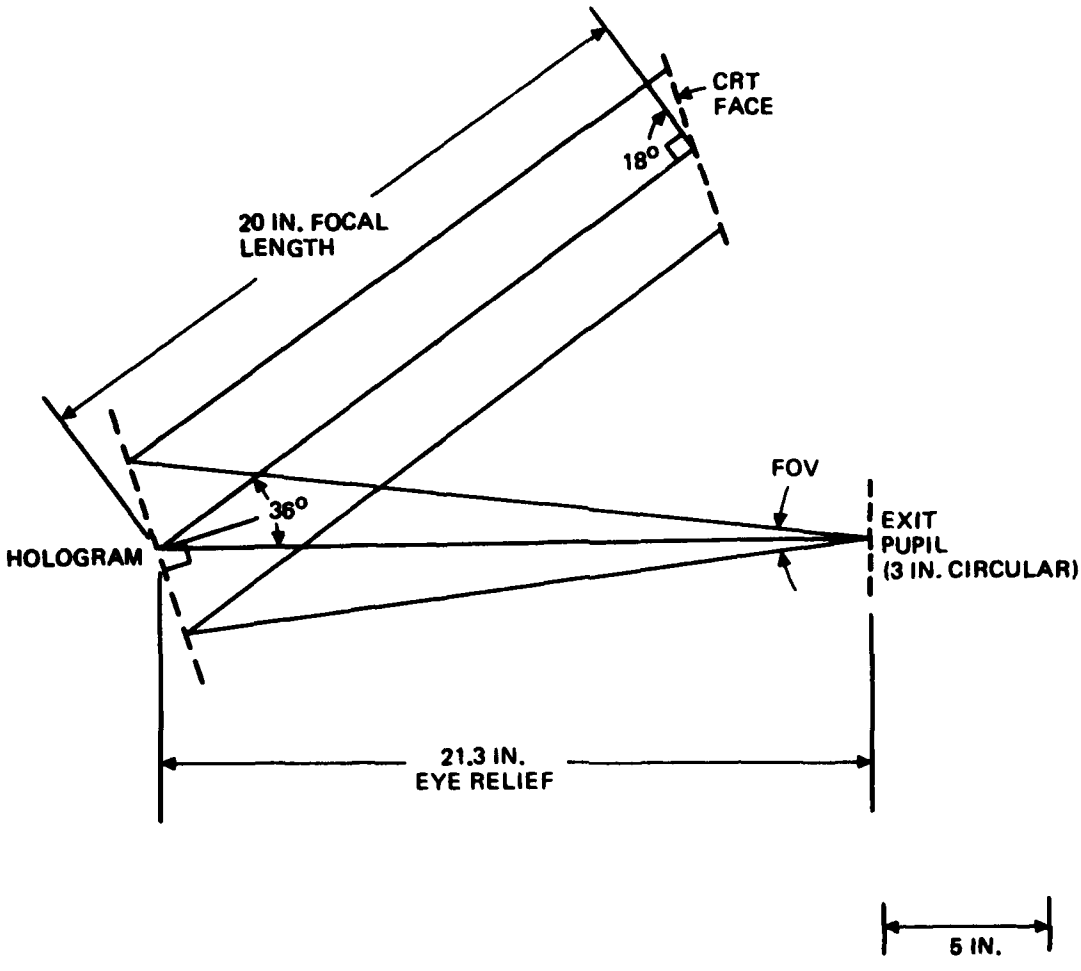

Figure 22. Relayless HHUD display geometry using the 36° off-axis, symmetric reflection hologram lens.

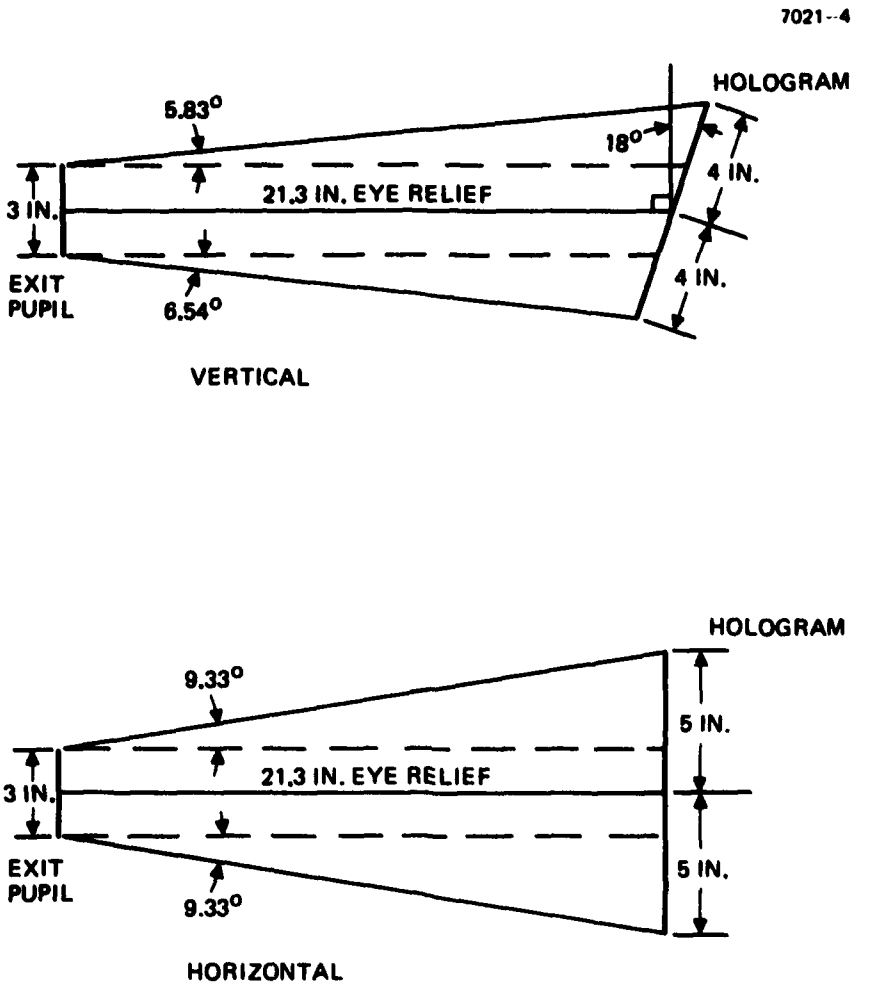

Figure 23. Vertical and horizontal FOV of the relay-less HHUD.

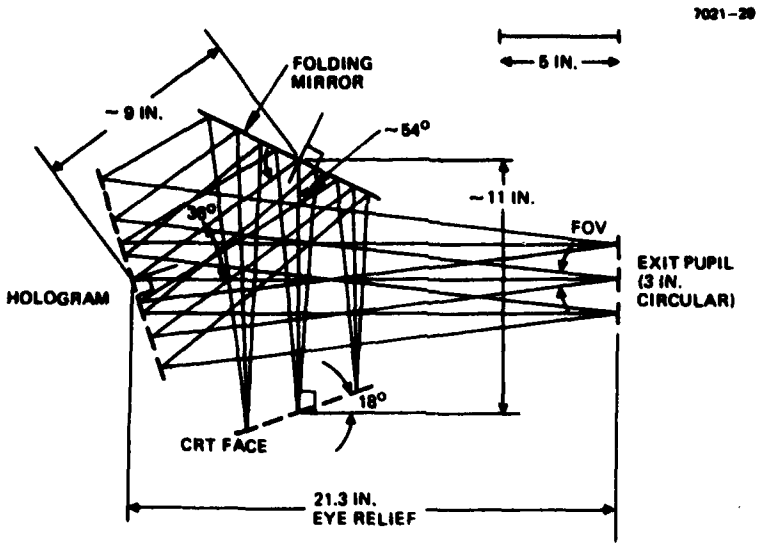

Figure 24. Alternate display geometry A for the relayless HHUD.

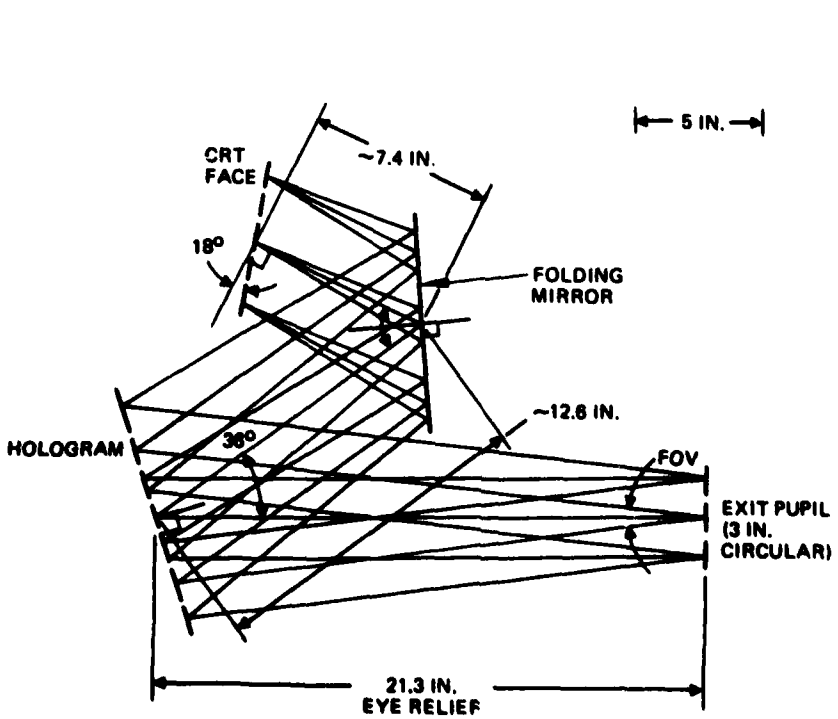

Figure 25. Alternate display geometry B for the relayless HHUD.

5. Efficiency and Losses

Axial efficiency and losses of holographic lenses laminated between two broadband AR-coated glass substrates were measured on a Cary 14 spectrophotometer from 4500 Å to 6500 Å wavelength. Optical density measured by the instrument is used to calculate efficiency ($\eta = 1 - 1/10^{(\text{efficiency OD})}$) and loss ($L = 1/10^{(\text{Loss OD})}$).

The characteristics of the delivered holographic lens are summarized in Figure 26 and Table 6. Measurements were taken by directing the interrogating beam along the axial ray of the hologram at 18° incident angle. At the operating wavelength (5430 Å) of the P-43 phosphor CRT (Figure 27), efficiency of the lens is ∿75%. Because of age and the hostile environment, holographic lenses will drift toward shorter wavelengths as spacing decreases. The efficiency (>75%) is maintained for 200 Å of drift. Environmental tests have projected insignificant wavelength drifts at room temperature for a period of several years.

Losses are caused by absorption and scatter of substrates (0.25 in. glass substrate/0.125 in. glass cover), epoxy, and DCG. Residual reflections from the glass substrate and cover added to the holographic lens losses. These losses, not due to the holographic lens, were measured by measuring substrate areas where no lens was exposed. Measured values ranged from 21% at the red end of the spectrum to 31% at the blue. The cause of this absorption is the plate glass tint. Due to manufacturing processes, float plate glass has smooth optical surfaces but a characteristic green hue. Optically clear glass (rolled) is available commercially but requires optical polishing to remove surface roughness.

The difference between the baseline measurement of hologram efficiency and the loss curve is caused by hologram absorption and scatter. Losses caused by the hologram ranged from 7% to 9%. These losses are attributed primarily to reflections off the cylindrical lenses used in the construction beams; the reflected beams produced extraneous exposure of the recording material, producing scattering. These lenses were AR-coated for low reflectivity at the red wavelength of the krypton laser used in Phases 2 and 3 of the program, and so had significant reflectivity at 5145 Å.

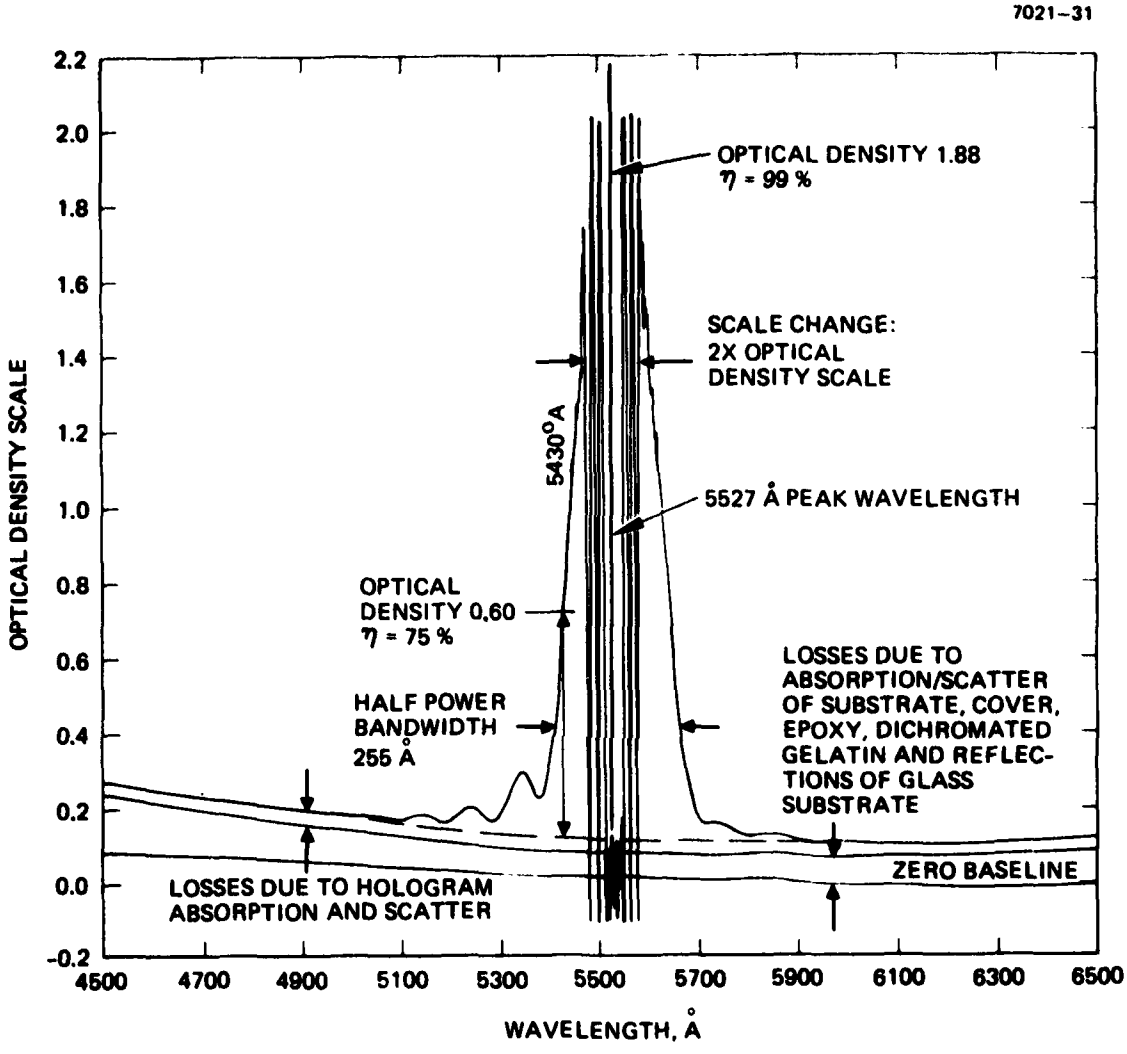

Figure 26. Efficiency and losses of 36° off-axis, symmetric reflection hologram lens.

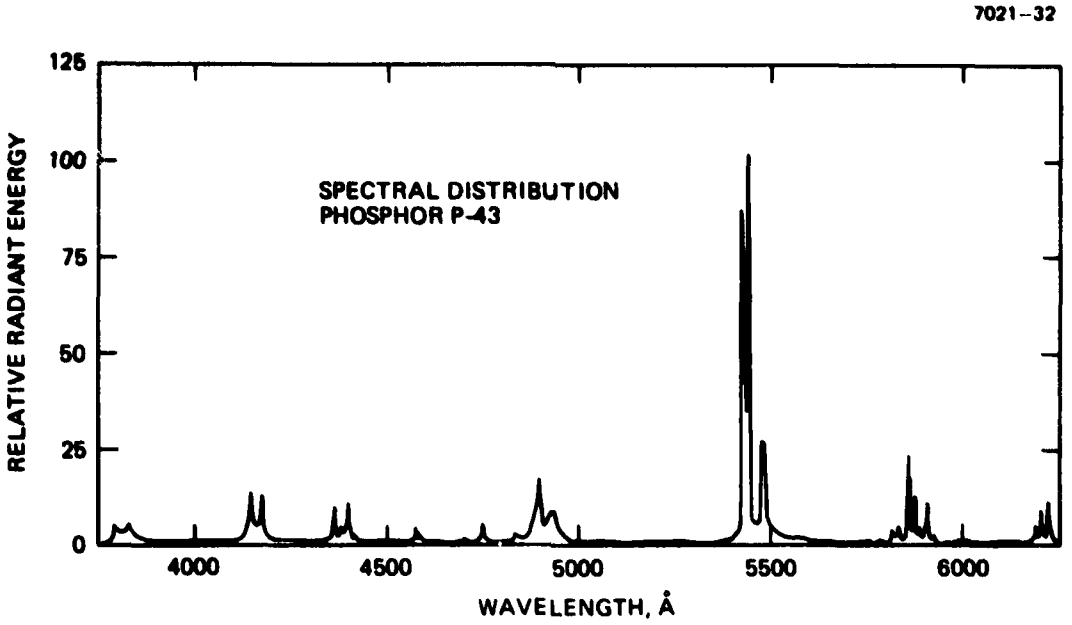

Figure 27. Spectral output of the P43 phosphor CRT.

Table 6. Summary of Hologram Efficiency and Loss Data.

	Measurement Wavelength			
	6500 Å	5527 Å	5430 Å	4500 Å
Losses caused by substrate absorption and scatter (1/4 in. glass), cover glass absorption and scatter (1/8 in. glass), epoxy, dichromated gelatin and residual glass reflections	21%		13%	31%
Losses caused by hologram absorption and scatter	7%		9%	9%
Total Losses	26%		21%	37%
Hologram efficiency at peak wavelength		99%		
Hologram efficiency at operating wavelength			75%	
Hologram half power bandwidth is 255 Å.				

6029

SECTION 5

REFLECTION HOLOGRAM ENVIRONMENTAL TEST

The usefulness of a holographic lens depends on its ability to withstand operational user environments without changing its optical properties. During this program, environmental tests were conducted on representative holograms. These demonstrated the basic compatibility of the planned head-up combiner with the military aircraft environment. Detailed test conditions and the resultant performance of the holographic lenses are discussed in this section.

The major parameters by which holographic lens performance can be assessed are diffraction efficiency, peak wavelength of reflectivity, and light scattering or absorption loss. For each of the environmental tests, these parameters were quantitatively measured in a Carry 14R spectrophotometer. The holograms were tested in their final form, having been holographically exposed, developed, and protected by a clear adhesive and cover glass.

A. EXPOSURE TO SUNLIGHT

Since a holographic head-up combiner is expected to be exposed to sunlight, we periodically compared the performance of two similar hologram lens samples — one placed on a white air conditioning intake duct on a roof at HRL, the other placed indoors. Semi-weekly measurements showed that the holographic properties of the two samples were very similar, and no deterioration of the sunlight exposed sample was recorded. This test continued for 14 months, and it implies an indefinite lifetime of these samples with respect to sunlight photodegradation limitations.

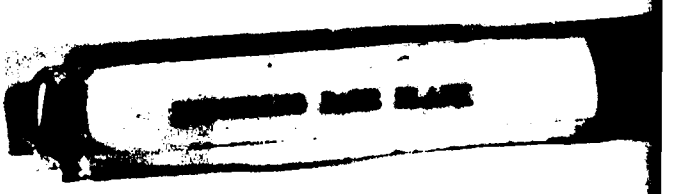

B. EXPOSURE TO 100% RELATIVE HUMIDITY

The 100% relative humidity test was conducted by immersing a sealed holographic lens for 4 hr in room-temperature water. After removal and drying, measurements showed no change in the hologram's optical properties. The same results were obtained when the test was repeated.

C. EXPOSURE TO HIGH TEMPERATURES

Three categories of high-temperature tests were performed:

- Performance of the hologram at room temperature after high-temperature cycling (as after hot storage).
- Determination of destructive temperature (as might be encountered in a parked, sunlit airplane cockpit).
- Performance of the hologram during temperature cycling (as might be encountered in hot, sunlit airborne environments).

1. High-Temperature Cycling

Performance of holographic lenses after high-temperature cycling was measured on 13 samples, processed in three different batches. The samples were measured before the test, placed in a recirculating air oven having close temperature control, and held at 80°C for over 720 hr. Measurements were taken at room temperature daily for the first week, then semi-weekly thereafter. Depending on the preparation methods and film-processing techniques, the samples showed wavelength drifts of 1 nm in 94 hr, 220 hr, and >560 hr. The slowest drift samples averaged about 1 nm drift in 800 hr at 80°C heating. Since we estimate that holographic lens performance would not be affected with 2 nm drifts, the high-temperature lifetime would exceed 1600 hr. All of the interrelated factors that may affect wavelength drift are complex because of the intricacy of the DCG recording process, and all possibilities have not been fully explored. However, extensive testing has been completed. These

tests permit predicting holographic lens lifetime for any given temperature. The important result is that a procedure has been developed that permits fabricating a hologram with a lifetime of about 1,600 hr at 80°C. For lifetime at other temperatures, an experimentally determined approximation (lifetime increases by a factor of 2.2 for each 10°C drop in temperature from 80°C) can be used. The total combiner lifetime would then be determined by an integration of its anticipated time versus temperature history. For a lifetime of 1,600 hr at 80°C, the lifetime at reduced temperatures is anticipated to be 9.4 years at 30°C (or 20.7 years at 20°C). Diffraction efficiency and optical clarity did not change by the baking cycles.

2. Destruction Temperature

The destructive temperature tests were performed on two hologram lenses by placing the samples in a baking chamber that had been stabilized at the test temperature. After a 2 hr bake, the samples were removed, allowed to come to room temperature, and then measured. The temperature was started at 20°C and raised in increments of 10°C until the hologram was destroyed. The two samples tested began to show significant wavelength shifts (i.e., shifts greater than 1 nm) at 100°C, although the diffraction efficiency remained constant. There was no significant wavelength shift up to that temperature. With continued testing at higher temperatures, the first sample failed at 130°C and the second sample failed at 140°C. Sample failure was manifest in the disappearance of the hologram, leaving a clear film layer. These tests show that the hologram is capable of withstanding environmental temperatures up to at least 100°C.

3. High-Temperature Operation

To measure the high-temperature operating condition of the hologram lens, a sample was wrapped with heating tape, then with insulating material. A small area in the center of the hologram was left open for continuous monitoring of the peak wavelength and diffraction

efficiency. Measurements were taken at approximately 5°C intervals from room temperature to 84°C. The heater was then shut off and measurements were taken until the sample cooled to 56°C, as shown in Figure 28. Within the estimated probable error in measurement (3 Å), the peak hologram reflection wavelength was constant. After cooling, however, a slight hysteresis was observed at the higher temperatures. This was probably caused by the shift in the measurement geometry that resulted from oxidation and contraction of the asbestos tape used to hold everything together during the bake cycle. Therefore, we conclude that the hologram lens does not change its optical properties with increasing temperature up to at least 84°C.

D. OTHER ENVIRONMENTAL TESTS

Other environmental tests included a cold soak and simultaneous exposure to high altitude and high temperature. In the cold soak test, two representative hologram samples were chilled from 20°C to -78.5°C for a minimum of 2 hr. No change of any kind was detected in these samples. In the second test, a sample was simultaneously subjected to a high-altitude atmosphere (approximating a 65,000 ft altitude) and a temperature of 55°C for 8 hr. The sample, after being removed from the test chamber, was measured for optical performance. No change from pre-test performance was observed.

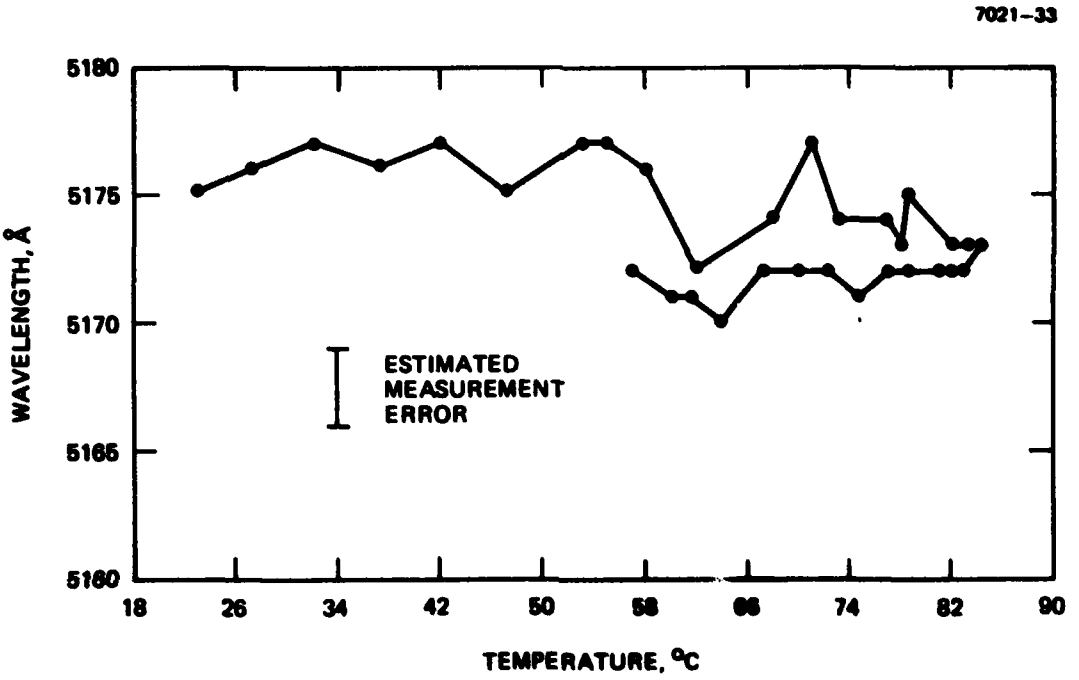

Figure 28. Hologram reflective wavelength as a function of ambient temperature for a sequential heating and cooling cycles.

REFERENCES

1. "Specification of Hologram Lens System," Naval Air Development Center, Air Vehicle Technology Department, 20 November 1972.

2. Final Technical Report for period 2 April 1973 - 1 April 1974, Contract N62269-73-C-0388, "Holographic Lens for Pilot's Head-Up Display," prepared for Naval Air Development Center, Warminster, PA 18974, by Hughes Research Laboratories, Malibu, CA 90265, D.H. Close, A. Au, and A. Graube, August 1974.

3. Final Technical Report for period 1 July 1974 - 31 October 1974, Contract N62269-74-C-0642, "Holographic Lens for Pilot's Head-Up Display," prepared for Naval Air Development Center, Warminster, PA 18974, by Hughes Research Laboratories, Malibu, CA 90265, D. H. Close, A. Au, and A. Graube, 1 April 1975.

4. Final Technical Report for period 18 March 1975 - 17 September 1975, Contract N62269-75-C-0299, "Holographic Lens for Pilot's Head-Up Display," prepared for Naval Air Development Center, Warminster, PA 18974, by Hughes Research Laboratories, Malibu, CA 90265, A. Au, A. Graube, and L. G. Cook, 1 February 1976.

5. T. A. Shankoff, "Phase Holograms in Dichromated Gelatin," Applied Optics 7, 2101 - 2105, (1968).

6. G. E. Moss, "Wide Angle Holographic Lens for a Display System," J. Opt. Soc. Am. 64, 552A, April 1974.